

General topological features and instanton vacuum in quantum Hall and spin liquids

A.M.M. Pruisken

*Institute for Theoretical Physics, University of Amsterdam,
Valckenierstraat 65, 1018 XE Amsterdam, The Netherlands.*

R. Shankar and Naveen Surendran*

The Institute of Mathematical Sciences, CIT Campus, Chennai 600 113, India.

We introduce the concept of *super universality* in quantum Hall liquids and spin liquids. This concept has emerged from previous studies of the quantum Hall effect and states that all the fundamental features of the quantum Hall effect are generically displayed as *general topological features* of the θ parameter in nonlinear σ models in two dimensions.

To establish super universality in spin liquids we revisit the mapping by Haldane who argued that the anti ferromagnetic Heisenberg spin s chain in $1+1$ space-time dimensions is effectively described by the $O(3)$ nonlinear σ model with a θ term. By combining the path integral representation for the dimerized spin $s = 1/2$ chain with renormalization group decimation techniques we generalize the Haldane approach to include a more complicated theory, the *fermionic rotor chain*, involving four different renormalization group parameters. We show how the renormalization group calculation technique can be used to lay the bridge between the *fermionic rotor chain* and the $O(3)$ nonlinear σ model with the θ term.

As an integral and fundamental aspect of the mapping we establish the topological significance of the *dangling spin* at the edge of the chain. The edge spin in spin liquids is in all respects identical to the *massless chiral edge excitations* in quantum Hall liquids. We consider various different geometries of the spin chain such as open and closed chains, chains with an *even* and *odd* number of sides. We show that for each of the different geometries the θ term has a distinctly different physical meaning. We compare each case with a topologically equivalent quantum Hall liquid.

PACS numbers: 73.43.-f, 75.10.Jm, 11.10.Kk, 64.60.Ak

I. INTRODUCTION

The topological concept of an instanton vacuum in scale invariant theories is one of the outstanding strong coupling problems in physics that to date has generally not been understood¹. Perhaps the most interesting and profound application of this concept is found in the theory of the *Quantum Hall Effect* (QHE)². The otherwise somewhat obscure *instanton angle* θ has a clear physical significance in this case. It represents a physical observable, namely the *Hall conductance*.

The advances^{3,4} made over many years have resulted in a clear physical understanding of the θ dependence in the Grassmannian $U(M+N)/U(M) \times U(N)$ non-linear σ model (NLSM) in terms of quantum Hall physics. In dramatic contrast to the standard lore which states that in this problem the *replica limit* (i.e. $M, N \rightarrow 0$) is all-important, one can now say that the fundamental features of the QHE are all displayed as *super universal topological features* of the *instanton vacuum*, independent of the details such as the number of field components (*replica's*) M and N in the theory. The list of super universal topological features includes the existence of *gapless excitations* at $\theta = \pi$, the appearance of *massless chiral edge excitations* as well as the existence of *robust topological quantum numbers* that explain the *observability* and *precision* of the QHE. These fundamental strong coupling aspects of the instanton vacuum should not be confused with the concept of *ordinary universality*. Ordinary universality applies solely to the details of the critical behaviour at $\theta = \pi$ which may in principle vary as one varies the number of field components in the theory. Following the standard phenomenology of critical phenomena one may associate different universality classes with different values of M and N . The various different aspects of the Grassmannian $U(M+N)/U(M) \times U(N)$ theory with varying values of M and N are encapsulated in the renormalization group flow diagrams of Fig. I. The *super universal* features are represented by the infrared stable fixed points at $\theta = 2\pi k$, as well as the unstable fixed points at $\theta = \pi(2k+1)$ which generally describe *gap-less* excitations or a *divergent* correlation length in the bulk of the system.

It is important to emphasize that the discovery of massless edge excitations has a major impact on our general

* Present Address: *Institute for Theoretical Physics, University of Amsterdam, Valckenierstraat 65, 1018 XE Amsterdam, The Netherlands.*

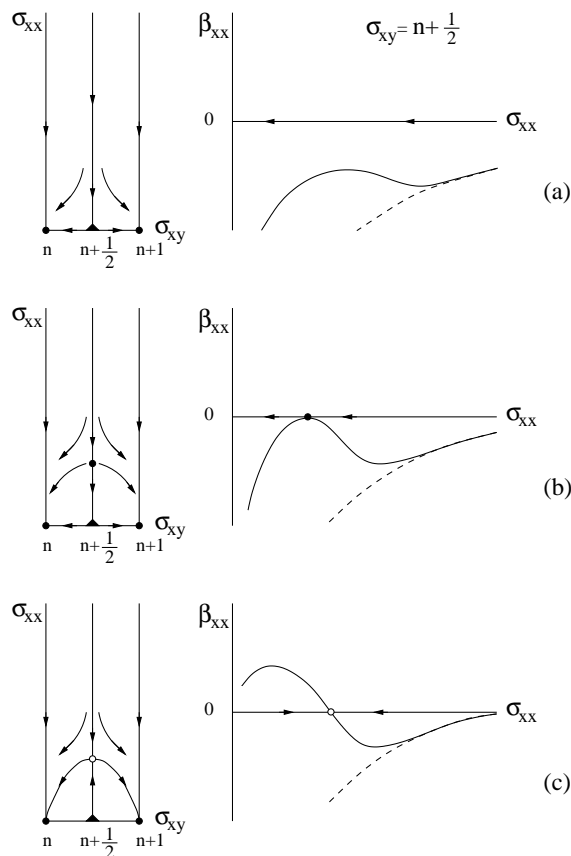


FIG. 1: The renormalization group flow diagram for different values of M and N in the σ_{xx} , σ_{xy} conductance plane. Here, $\sigma_{xx} = 1/2g$ and $\sigma_{xy} = \theta/2\pi$ where g denotes the coupling constant and θ the instanton angle. (a) The unstable fixed points along the lines $\sigma_{xy} = n + 1/2$ may have a critical value $\sigma_{xx}^* = 0$ as found in the large N expansion of the CP^{N-1} model or, equivalently, $SU(N)/U(N-1)$. (b) The value σ_{xx}^* is finite but with a *marginally irrelevant* direction ($\sigma_{xx} > \sigma_{xx}^*$) and a *marginally relevant* ($\sigma_{xx} < \sigma_{xx}^*$) direction respectively. This behaviour is expected for $M = N = 1$ or $SU(2)/U(1) \simeq O(3)$. (c) The critical point has a finite σ_{xx}^* and is stable along the entire $\sigma_{xy} = n + 1/2$ axis. This behaviour is typical for the theory with a small number of field components $1 \gtrsim M, N \geq 0$.

understanding of the instanton vacuum at strong coupling^{5,6}. It has resulted in a fundamental revision³ of commonly accepted but conflicting ideas and expectations that were all based on extended previous work on an “exactly” solvable limit of the theory, the large N expansion of the CP^{N-1} model⁷. These historical analyzes have set the stage for the θ dependence in an overwhelming majority of Grassmannian $U(M+N)/U(M) \times U(N)$ NLSM’s, presumably all integers M and N larger than unity, for which the physics at large distances is likely to be the same. Assuming the historical results and claims to be true, however, then none of the aforementioned super universal features of the instanton vacuum would actually exist. This dramatic conflict between the historical claims and the physics of the QHE has spanned the subject of an instanton parameter θ for a very long time. It is just one of the reasons why it has proven to be so difficult in this field to pursue the right physical ideas as well as the appropriate mathematical questions.

It so turned out that much of the historical large N analysis is fundamentally incorrect³. For one thing, the topological subtleties of the “edge” in this problem have been entirely overlooked and, along with that, the most relevant part of the excitation spectrum, namely the *gap-less* bulk excitations that generally exist at $\theta = \pi$. Much of the dilemma is due to the fact that although the topological phase transition at $\theta = \pi$ may formally be a *first order* one, the system can nevertheless exhibit a diverging correlation length and, hence, display all the characteristics of a *continuous, second order transition*. In any case, in dramatic contrast to what the historical analyzes were saying or trying to say, the large N expansion, as it now stands, is one of the very rare and interesting examples where the super universal strong coupling features of the instanton vacuum concept can be fully explored and demonstrated in great detail.

In this paper we investigate the *super universality* concept in a somewhat different physical context, the one dimensional anti-ferromagnetic Heisenberg spin chain (HSC). In 1983 Haldane⁸ argued that the HSC, in the limit of

large spin s , is effectively described by the $SU(2)/U(1) \simeq O(3)$ NLSM with a θ term. On the basis of this mapping (in brief *Haldane mapping*) Haldane predicted that the HSC with $s = 1$ has a mass gap whereas for $s = 1/2$ the chain is known to be gapless. Subsequently, Affleck⁹ extended the argument to include the *dimerized Heisenberg spin chain* (DSC). For the DSC the parameter θ becomes, like in the theory of the QHE, a continuously varying parameter. The relevant variable in the case is the so-called *dimerization parameter* κ .

As a general remark we can say that Haldane conjecture for spin chains naturally emerges from the renormalization group flow diagram as it was obtained from the studies of the QHE (Fig. 1b). In so far as one can trust the Haldane mapping for more complicated situations such as the DSC for arbitrary s , dimerized $SU(N)$ spin chains etc., one proceed along similar lines and obtain the global phase diagram of the spin system from the flow diagram of the corresponding NLSM.

Unfortunately, the Haldane mapping has in general not been understood well enough to facilitate an unambiguous, one-to-one mapping between the spin chain and continuum field theory, i.e. the NLSM in the presence of the θ term. While the theory near the $\theta = \pi$ ($\kappa = 1$) has been extensively studied in the context of both the DSC¹⁰ and the $O(3)$ NLSM¹¹ nobody has as of yet recognized that both models display all the fundamental strong coupling features of the QHE. The complications in the Haldane mapping are clearly reflected by the fact that even to date some unresolved issues have remained such as the difference between spin chains with an *even* and an *odd* number of spins. A related problem is the peculiar role played by the *dangling spin* at the edge of the chain. In all these cases it is not quite understood how the Haldane mapping should be carried out, or what the θ term in the $O(3)$ NLSM actually stands for. In face of the various approximation schemes that are involved such as the large s expansion, the continuum limit etc. it is not always clear which features of the quantum spin chain are captured by continuum field theory and which are due to, say, the lattice.

The principal objective of this paper is to revisit the Haldane mapping of the DSC and investigate whether it can be used, like the large N expansion of the CP^{N-1} model, as an explicit example for demonstrating the super universal features of the instanton vacuum. We are interested, in particular, in the specific mechanism that is responsible for the generation of *robust* topological quantum numbers, i.e. the QHE itself.

In order to achieve our goals we shall begin in Section II with a review of edge excitations in the Grassmannian NLSM as well as the simple example of a single Heisenberg spin in a magnetic field B . From the *path integral representation* (PIR) we readily establish the fact that the dynamics of the isolated spin is exactly described by the θ term (solid angle term) that one normally would associate with the $O(3)$ NLSM. The time correlations that we obtain precisely correspond to those obtained earlier, describing the *massless chiral edge modes* in quantum Hall systems. This clearly indicates that the *dangling spins* at the edge of the chain, just like the *edge currents* in quantum Hall systems, are responsible for the low energy dynamics of the instanton vacuum in strong coupling. It is important to remark, though, that our phrase “edge correlations” is not obviously related to the *chiral edge boson* approach in $1 + 1$ space-time dimensions that one usually associates with the QHE. Although one deals with essentially the same physical phenomenon, the formal equivalence between the two theories is by no means any obvious and the matter has been addressed in great detail in Refs⁵ and⁶.

The results for the single spin motivate us to proceed and investigate the Haldane mapping for spin chains with and without an edge in Section III. We consider the closed chain, open chains with an even/odd number of spins as well as the half infinite chain and establish their *topological differences*. These differences are reflected by the fact that for each case the θ parameter in the continuum field theory has a distinctly different physical meaning. For specificity we shall associate *topologically* distinct quantum Hall systems with each of the *geometrically* different spin chain in Section IV.

Armed with these insights we next address the various strong coupling aspects of the Haldane mapping in greater detail. We focus the attention primarily on the problem of *weakly coupled dimers* where one naively would expect that the Haldane mapping can no longer be trusted. To deal with this problem in all its generality we set up in Section V an *exact* renormalization group decimation scheme that can be applied directly to the PIR of the DSC. Here, the phrase *exact* means that in the limit of completely decoupled dimers the renormalization group equations can be systematically expanded order by order in the small dimerization parameter κ . The important advantage of this scheme is that it can be applied to all geometrically different spin chains under consideration (*open* and *closed* spin chains etc.).

Next we specify to the $s = 1/2$ case and obtain explicit results from the decimation procedure. These reveal several novel and important aspects of the problem that ultimately lay the bridge between the DSC and continuum field theory.

1. First of all, the renormalization group takes us away from the pure DSC and the system “flows” into a more general dimerized chain, termed the fermionic rotor chain (FRC). Unlike the DSC, the FRC involves in total four different coupling constants $\kappa_1, \dots, \kappa_4$ rather than the dimerization parameter κ alone.
2. The renormalization group equations can be solved exactly, the solution indicating that the FRC has a *massive*

fixed point as expected. However, the mass gap of the FRC is actually a highly nonperturbative expression in the coupling constants.

3. The decimation procedure *dynamically* generates a *dangling spin* with $s = 1/2$ at the edge of the chain. The renormalization group procedure demonstrates explicitly that the spin at the edge becomes completely decoupled from the bulk only after a sufficiently large number of iterations.
4. Guided by the results of the decimation procedure we next derive in Section VI the NLSM in the presence of the θ term, describing the low energy dynamics of the FRC. The derivation proceeds analogous to the Haldane mapping. We make use of the fact that the two rotors on each dimer are almost anti-parallel. The deviation from being anti-parallel are then the “hard” fields which are integrated out. As the final step we perform the continuum limit which then leads to explicit expressions of the NLSM parameters (the coupling constant g and the instanton angle θ) in terms of the FRC parameters $\kappa_1, \dots, \kappa_4$.
5. At this stage of the analysis all the results that we have obtained become simultaneously important. First of all the renormalization group equations of the FRC directly imply that the NLSM parameters g and θ are *running* parameters with length scale. Hence, our results explicitly display the important feature of θ *renormalization*. Secondly, the effective NLSM action associated with the “massive” fixed points of the FRC precisely describes the time correlations of the *dangling spin* at the edge or, equivalently, *massless chiral edge excitations* in quantum Hall systems. Thirdly, the general renormalization group scenario that emerges, in the inverse coupling constant $1/g$ versus θ plane, explicitly demonstrates how the QHE emerges as a super universal strong coupling feature of the instanton vacuum. We identify the Hall conductance in the system and show that it is robustly quantized with corrections that are exponentially small in the size of the chain. We end this paper with a conclusion in Section VII.

II. PHYSICS AT THE EDGE

A. The strong coupling limit

Within the replica field theory approach to localization problems the low energy dynamics of quantum Hall regime is described by the Grassmannian $U(N + M)/U(N) \times U(M)$ NLSM. The effective action is defined as follows²

$$\begin{aligned}
 S[Q] = & -\frac{1}{8}\sigma_{xx}^0 \int d^2x \text{tr}(\nabla Q)^2 \\
 & +\frac{1}{8}\sigma_{xy}^0 \int d^2x \text{tr} \epsilon_{ij} Q \partial_i Q \partial_j Q \\
 & +\pi\rho_0\omega \int d^2x \text{tr} \Lambda Q.
 \end{aligned} \tag{1}$$

The field variable $Q(x)$ can be represented according to

$$Q = T^{-1} \Lambda T, \quad T \in U(N + M) \tag{2}$$

where Λ is a diagonal matrix with N diagonal elements equal to 1 and the other M equal to -1

$$\Lambda = \begin{pmatrix} \mathbf{1}_N & 0 \\ 0 & -\mathbf{1}_M \end{pmatrix}. \tag{3}$$

The results for the electron gas are obtained by taking the *replica limit* $N, M \rightarrow 0$ at the end of all computations. As mentioned earlier, the coupling constants σ_{xx}^0 and σ_{xy}^0 are dimensionless quantities representing the mean field *longitudinal* and *Hall* conductances respectively. The quantity ρ_0 is the density of electronic levels and ω is the external frequency that is normally used to regulate the infrared of the system.

To study the theory in the DC limit ($\omega = 0$) we have to specify the boundary conditions satisfied by the Q fields. As always, this has to be decided by the physics of the system under consideration. It was shown^{3,4,5,6} that “free” boundary conditions (i.e. no boundary conditions on the matrix field variables Q) implies the existence of *massless chiral edge excitations*. In this Section we briefly review these ideas and show that they resolve some of outstanding strong coupling problems associated with the topological concept of an instanton vacuum.^{3,4}

1. Fractional topological charge and chiral edge excitations

The most important consequence of free boundary conditions is that the topological charge $\mathcal{C}[Q]$ of the theory is not quantized. By writing an arbitrary matrix field Q as follows,

$$Q = t^{-1}Q_0t, \quad (4)$$

where Q_0 has a fixed value at the edge, say Λ , and t represents the fluctuations about these special boundary conditions. Then in general we can write,

$$\mathcal{C}[Q] \equiv \frac{1}{16\pi i} \int d^2x \operatorname{tr} \epsilon_{ij} Q \partial_i Q \partial_j Q \quad (5)$$

$$= \mathcal{C}[Q_0] + \mathcal{C}[q]. \quad (6)$$

Here, $\mathcal{C}[Q_0]$ is by construction *integer* quantized. The quantity $\mathcal{C}[q]$ with $q = t^{-1}\Lambda t$ represents the *fractional* part and without loss of generality we can write $-1/2 \leq \mathcal{C}[q] < 1/2$.

The fundamental significance of the fractional charge $\mathcal{C}[q]$ becomes particularly transparent if we consider the special case where the Fermi energy of the electron gas lies in a Landau gap. Examining this physical situation is important since it corresponds to the naive strong coupling limit of the theory obtained by putting $\sigma_{xx}^0 = \rho_0 = 0$ and $\sigma_{xy}^0 = k$ with the integer k denoting the number of completely filled Landau bands. The action becomes simply

$$S[Q] = \frac{k}{8} \int d^2x \operatorname{tr} \epsilon_{ij} Q \partial_i Q \partial_j Q \quad (7)$$

which can be written as

$$S[Q] = 2\pi i k \mathcal{C}[Q_0] + \frac{k}{2} \oint d\vec{x} \cdot \operatorname{tr}(\Lambda t \nabla t^{-1}) \quad (8)$$

The significance of the integer valued Hall conductance $\sigma_{xy}^0 = k$ is now clear. In particular, since $\sigma_{xx}^0 = 0$ the theory renders completely insensitive to the field configurations Q_0 that have an *integer quantized* topological charge. These configuration are generally identified as the *bulk excitations* of the theory. The action solely depends only on the fluctuating matrix fields t along the one dimensional edge of the system. Hence, one can generally identify the *edge excitations* of the system with those matrix field configurations that carry a *fractional* topological charge.

It turns out that the complete expression for the effective action along the edge is given by^{3,4}

$$S[t] = \frac{k}{2} \oint d\vec{x} \cdot \operatorname{tr}(\Lambda t \nabla t^{-1}) + \omega \rho_{edge} \operatorname{tr} \Lambda q. \quad (9)$$

Here, the quantity ρ_{edge} indicates that although the density of levels is zero in the *bulk* there nevertheless exists a finite density of electronic levels at the *edge* of the system that can carry the Hall current.

2. Chiral edge fermions and chiral edge bosons

It should be emphasized that the action for the *edge* (Eq. 9) was originally obtained as a special case of a *bulk* theory that does not involve any explicit knowledge on the microscopic details of the edge of the electron gas.² It can remarkably be shown, however, that Eq. (9) is completely equivalent to a system of disordered *chiral fermions* that are confined at the edge of the system.³ The replicated chiral fermion action S_{CF} is given in terms of k independent edge modes according to

$$S_{CF}(V) = \int \sum_{jj'=1}^k \operatorname{tr} \Psi_j^\dagger \left[-iv_d \partial_x + V^{jj'} + i\omega \Lambda \right] \Psi_{j'}. \quad (10)$$

Here, Ψ_j and Ψ_j^\dagger represent $(N + M)$ -component vectors of fermion fields which can be written as $[\psi_{j\alpha}^{(+)}(x), \psi_{j\beta}^{(-)}(x)]$ and $[\bar{\psi}_{j\alpha}^{(+)}(x), \bar{\psi}_{j\beta}^{(-)}(x)]^\dagger$ respectively with $\alpha = 1, 2, \dots, N$ and $\beta = 1, 2, \dots, M$. The hermitian matrices $V^{jj'}(x)$ are randomly distributed potentials (with a Gaussian weight) that facilitate scattering between the edge channels labeled by j and j' .

The equivalence of Eqs (10) and (9) can formally be demonstrated on the basis of the standard techniques using the Hubbard-Stratonovich transformation. However, an important aspect of chiral electrons is that the quenched randomness such as $V^{jj'}$ can be “gauged away”. This means that the “gauge invariant” correlations of the system can be computed in a trivial and exact manner simply by putting the random matrices $V^{jj'}$ in Eq. (10) equal to zero. Several important examples are as follows³

$$\langle q_{\alpha\beta}^{pp'}(x) \rangle_q = \rho_{edge}^{-1} \sum_{j=1}^k \langle \bar{\psi}_{j\alpha}^p(x) \psi_{j\beta}^{p'}(x) \rangle_{CF} = (\Lambda)_{\alpha\beta}^{pp'}. \quad (11)$$

Here, the expectations $\langle \dots \rangle_q$ and $\langle \dots \rangle_{CF}$ are with respect to the theory of Eq. (9) and Eq. (10) with $V^{jj'} = 0$ respectively. Furthermore, we have made use of the following relation between the density of edge levels ρ_{edge} and the drift velocity v_d of the chiral electrons

$$\rho_{edge} = m/v_d. \quad (12)$$

Eq. (11) surprisingly shows that the continuous $U(N+M)/U(N) \times U(M)$ symmetry is *permanently broken* at the edge of the system, independent of the values of N and M . The higher order correlation functions can be computed along similar lines. The only non-vanishing two point function is given by³

$$\begin{aligned} & \langle q_{\alpha\beta}^{-+}(x) q_{\alpha\beta}^{+-}(y) \rangle_q \\ &= \rho_{edge}^{-2} \sum_{jj'=1}^k \langle \bar{\psi}_{j\alpha}^{(-)}(x) \psi_{j\beta}^{(+)}(x) \bar{\psi}_{j'\alpha}^{(+)}(y) \psi_{j'\beta}^{(-)}(y) \rangle_{CF} \end{aligned} \quad (13)$$

$$= k\vartheta(x-y)e^{-2\omega\rho_{edge}(x-y)} \quad (14)$$

for $x \neq y$ and ϑ denoting the Heaviside step function. This result clearly shows that in the limit $\omega = 0$ the theory is length scale independent and, hence, our one dimensional edge theory is a *critical theory*.

In summary we can say that the instanton vacuum displays *massless chiral edge excitations*. This remarkable and exactly solvable feature is independent of the number of field components (replica's) N and M in the theory. We have focused so far on the “naive” strong coupling limit of the theory which in the language of the electron gas corresponds to the very special case of integer filling fractions $\nu = k$ where the system displays an energy gap or *Landau gap*. In the next Section we will show, however, that the result of Eq. (9) actually has a much broader range of validity and quite generally emerges as the *critical fixed point action* of the quantum Hall state. Although experimentally well established, the quantum Hall state says something highly non-trivial and remarkably general about the strong coupling features of the instanton vacuum concept that previously have remained concealed.

3. Quantization of the Hall conductance

To address the theory in all its generality it is necessary to find a way in which the massless edge modes t are unambiguously separated from the distinctly different bulk matrix field variables Q_0 . This separation becomes immediately transparent once it is recognized that the mean field quantity σ_{xy}^0 can generally be expressed as the sum of an *integer quantized* “edge” piece k and an *unquantized* “bulk” piece θ_{bulk} . Working for simplicity in the limit of strong magnetic fields B then σ_{xy}^0 is identical to the filling fraction² ν such that we can write

$$\sigma_{xy}^0 \equiv \nu = k(\nu) + \theta_{bulk}(\nu)/2\pi. \quad (15)$$

where

$$k(\nu) \in \mathbb{Z}, \quad -\pi \leq \theta_{bulk}(\nu) < \pi \quad (16)$$

In Fig. 2 we sketch the $k(\nu)$ and $\theta_{bulk}(\nu)$ with varying ν . To see how the split in Eq. (15) facilitates a general discussion of the theory on the strong coupling side we first consider the topological piece of the action which now can be written as follows

$$\begin{aligned} & \frac{1}{8}\sigma_{xy}^0 \int \text{tr} \epsilon_{ij} Q \partial_i Q \partial_j Q = 2\pi i \sigma_{xy}^0 \mathcal{C}[Q] \\ &= 2\pi i \{k(\nu) + \theta_{bulk}(\nu)/2\pi\} \{\mathcal{C}[Q_0] + \mathcal{C}[q]\} \\ &= 2\pi i k(\nu) \mathcal{C}[q] + i\theta_{bulk}(\nu) \mathcal{C}[Q]. \end{aligned} \quad (17)$$

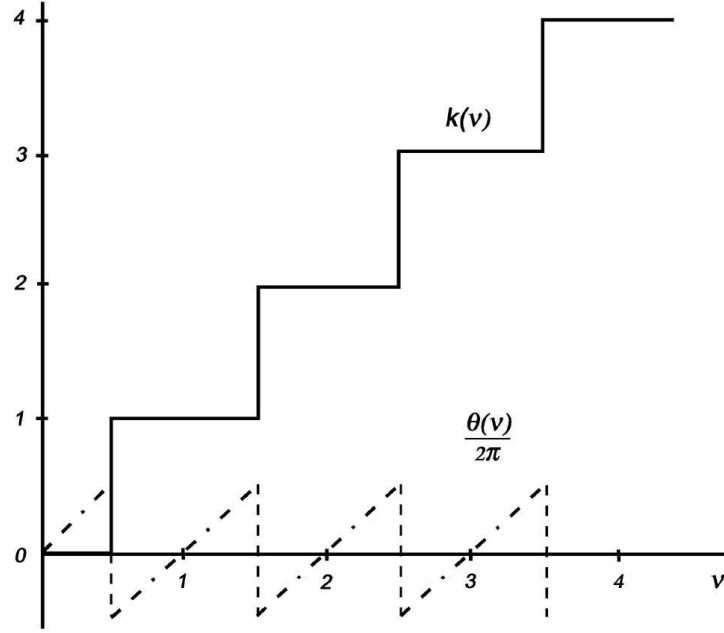


FIG. 2: The quantity $\sigma_{xy}^0 = \nu$ is the sum of a *quantized* edge part $k(\nu)$ and an *unquantized* bulk part $\theta(\nu)$.

In the last step we have left out the term $2\pi i k(\nu) \mathcal{C}[Q_0]$ since it gives rise to phase factors which are not of interest to us. On the basis of this result we can split the action $S[Q]$ into an edge piece and a bulk piece as follows

$$S[Q] = S_{edge}[q] + S_{bulk}[Q] \quad (18)$$

$$S_{edge}[q] = 2\pi i k(\nu) \mathcal{C}[q] = \frac{k(\nu)}{2} \oint \text{tr} t \partial_x t^{-1} \Lambda \quad (19)$$

$$S_{bulk}[Q] = -\frac{1}{8} \sigma_{xx}^0(\nu) \int \text{tr}(\nabla Q)^2 + i \theta_{bulk}(\nu) \mathcal{C}[Q]. \quad (20)$$

Notice that in the very special case of an integer valued filling fraction ν the bulk part of the action S_{bulk} is trivially equal to zero and we recover the results of the previous Section. On the other hand, to deal with the general situation of arbitrary ν we must perform the integration over the bulk matrix field variables Q_0 . Provided the edge matrix field variables q obey the classical equations of motion in the bulk of the system one can express the results in terms of an effective action

$$e^{S'_{bulk}[q]} = \int_{\partial V} D[Q_0] e^{S_{bulk}[t^{-1} Q_0 t]}. \quad (21)$$

The subscript ∂V reminds us of the fact that the functional integral has to be performed with a fixed value $Q_0 = \Lambda$ at the edge. Next, on the basis of very general symmetry considerations³ one concludes that the effective action $S'_{bulk}[q]$ has to be of the form

$$S'_{bulk}[q] = -\frac{1}{8} \sigma'_{xx} \int \text{tr}(\nabla q)^2 + i \theta'_{bulk} \mathcal{C}[q]. \quad (22)$$

The total effective action for the edge field variable q becomes

$$S_{eff}[q] = S'_{edge}[q] + S'_{bulk}[q] \quad (23)$$

$$= -\frac{1}{8} \sigma'_{xx} \int \text{tr}(\nabla q)^2 + 2\pi i (k(\nu) + \theta'_{bulk}/2\pi) \mathcal{C}[q]. \quad (24)$$

Here, the quantities σ'_{xx} and $\sigma'_{xy} = k(\nu) + \theta'_{bulk}/2\pi$ are identified as the macroscopic transport coefficients of the system, i.e. the Kubo formulae for the longitudinal and Hall conductance respectively.²

In spite of the fact that Eqs (21) and (22) are extremely complicated expressions as they stand, they nevertheless provide a profound and general framework that is needed for a microscopic understanding of the quantum Hall effect. For example, since the non-linear σ model is known to be asymptotically free in two dimensions for all non-negative integer values of N and M , one generally expects the theory to *dynamically* develop a mass gap in the limit of large distances. On the other hand, from the definition of σ'_{xx} and θ'_{bulk} we clearly see that these quantities play the role of *response parameters* that measure the sensitivity of the bulk of the system to an infinitesimal change in the boundary conditions. These quantities should therefore render exponentially small in the system size L provided the bulk of the system displays a mass gap or a finite correlation length (localization length) ξ . Putting the various different statements together we obtain the following general expressions for the quantum Hall effect

$$\sigma'_{xx} = \mathcal{O}(e^{-L/\xi}) \quad (25)$$

$$\begin{aligned} \sigma'_{xy} &= k(\nu) + \theta'_{bulk}/2\pi \\ &= k(\nu) + \mathcal{O}(e^{-L/\xi}). \end{aligned} \quad (26)$$

It now is clear why the critical edge excitations play such a fundamental role in this problem. Following Eq. (24) we see that the effective action of the quantum Hall state precisely equals the action for massless chiral edge excitations S_{edge} . This explains why the quantity $k(\nu)$ entering the expression for the Hall conductance (Eq. 26) is *length scale independent* and, hence, *quantized*. This is quite unlike the bulk part of the Hall conductance $\theta'_{bulk}/2\pi$ which probes the mass gap in the bulk of the system. This quantity therefore determines the *corrections* to exact quantization which, as mentioned above, are exponentially small in the system size.

Notice that nothing much of the argument seems to depend on the specific application of the instanton vacuum that one considers. One therefore expects that the theory generically displays the principal aspects of the quantum Hall effect, independent of the values of N and M . It is important to emphasize, however, that none of these general strong coupling features of the theory have previously been recognized, in particular the fundamental significance of θ *renormalization*. It is therefore extremely important to have certain explicit examples of an instanton vacuum where the statements of Eq. (26) can be explored and investigated in detail. The rest of this paper will be devoted to developing a formalism that enables us to analytically access the strong coupling quantum Hall fixed points.

We end this Section with several remarks. First of all, it should be mentioned that the statement of Eq. (15) has a quite general significance which is not limited to strong coupling phenomena alone. In fact, both the motivation and justification of the split in σ'_{xy} is provided by the detailed knowledge obtained from the “observable” parameters σ'_{xx} and θ'_{bulk} in the weak coupling regime. The results can generally be expressed in terms of renormalization group β functions according to ⁴

$$\sigma'_{xx} = \sigma_{xx}^0 + \int_{\lambda_0}^{\lambda'} \frac{d\lambda}{\lambda} \beta_{\sigma}(\sigma_{xx}, \theta_{bulk}) \quad (27)$$

$$\theta'_{bulk} = \theta_{bulk}^0 + \int_{\lambda_0}^{\lambda'} \frac{d\lambda}{\lambda} \beta_{\theta}(\sigma_{xx}, \theta_{bulk}). \quad (28)$$

Here, the λ' and λ_0 denote the length scales that are generally associated with the observable theory $\sigma'_{xx}, \theta'_{bulk}$ and bare theory $\sigma_{xx}^0, \theta_{bulk}^0 = \theta_{bulk}(\nu)$ respectively. By using otherwise very general statements of symmetry one can show that the β functions can be written in terms of an infinite trigonometric series in discrete topological sectors of the theory according to

$$\beta_{\sigma} = \frac{d\sigma_{xx}}{d \ln \lambda} = \sum_{n=0}^{\infty} f_n(\sigma_{xx}) \cos n\theta_{bulk} \quad (29)$$

$$\beta_{\theta} = \frac{d\theta_{bulk}}{d \ln \lambda} = \sum_{n=1}^{\infty} g_n(\sigma_{xx}) \sin n\theta_{bulk} \quad (30)$$

These results tell us that the lines $\theta_{bulk} = \pm\pi$ and $\theta_{bulk} = 0$ are invariant under the action of the renormalization group. On the other hand, an explicit computation of the lowest order terms in the series leads to the following results⁴

$$f_0(\sigma_{xx}) = -(N+M) - \frac{NM + N + M}{\sigma_{xx}} + \mathcal{O}(\sigma_{xx}^{-2}) \quad (31)$$

$$f_1(\sigma_{xx}) = 2\pi g_1(\sigma_{xx}) = -D_{N,M} \sigma_{xx} e^{-2\pi\sigma_{xx}} \quad (32)$$

where the positive quantity $D_{N,M}$ is determined by the instanton determinant.⁴ These results clearly indicate that the renormalization group flow is toward the strong coupling fixed point $\sigma_{xx} = \theta_{bulk} = 0$ which is stable in the infrared.

Notice that the β functions can also be written in terms of the Hall conductance σ_{xy} simply by replacing $\theta_{bulk}/2\pi$ by $k(\nu) + \theta_{bulk}/2\pi$. This leads to the well known statement which says that the renormalization group flow is *periodic* in σ_{xy} . This statement, however, is equivalent to the following statement which says that

$$\frac{dk(\nu)}{d \ln \lambda} = 0. \quad (33)$$

As we have seen earlier, the true justification of this result and, hence, of the aforementioned *periodicity* statement in the σ_{xx}, σ_{xy} conductance plane lies in the *critical* behavior of the edge of the instanton vacuum. This changes the meaning of Eq. (33) into that of a *critical fixed point*.

B. Edge spins

For the rest of this paper, we will focus on the $N = M = 1$ case. The group, $SU(N + M)$ is then $SU(2)$ and the Grassmannian is the 2-sphere. Q parameterizes the points on a 2-sphere and we can write it as,

$$Q = \hat{n} \cdot \vec{\tau} \quad (34)$$

Where \hat{n} is a unit vector. The fractional part of the θ term is the solid angle of the curve traced out on the sphere by \hat{n} as it goes around the edge. The action (7) can be written as,

$$S[Q] = is \int d^2x \hat{n} \cdot \partial_x \hat{n} \times \partial_y \hat{n} + 2\pi \rho_{edge} \omega n^3 \quad (35)$$

with $s = \frac{m}{2}$. This is exactly the action obtained for the problem of a spin- s system^{12,13}, if the Euclidean time of the spin system is identified with the coordinate that parameterizes the edge, say x . The other coordinate, y , that goes into the bulk plays the role of the fictitious dimension that it is necessary to introduce in the spin problem in order to write down a globally well defined action.

The path integral for spin systems is standardly derived using spin-coherent states^{12,13}. The spin- s system is an irreducible representation of the angular momentum algebra,

$$\begin{aligned} [J^a, J^b] &= i\epsilon^{abc} J^c \\ J^a J^a |\psi\rangle &= s(s+1) |\psi\rangle \end{aligned} \quad (36)$$

The states can be labeled by the eigenvalue of J^3 ,

$$J^3 |M\rangle = M |M\rangle, \quad M = -s, \dots, s \quad (37)$$

The spin coherent states are defined as,

$$|Q\rangle = T | -s \rangle \quad (38)$$

Where, $T \in SU(2)$. The little group of the state $| -s \rangle$ is $U(1)$. So the states are in one-to-one correspondence with points on the 2-sphere. They are labeled by $Q = -T\tau^3 T^{-1}$. If we take the Hamilton to be,

$$H = 4\pi \frac{\rho_{edge}}{2s} J^3 \quad (39)$$

Then the path integral representation for the partition function is,

$$Z = \text{tr} e^{-LH} \quad (40)$$

$$= \int \mathcal{D}[Q(x)] e^{-S[Q(x)]} \quad (41)$$

Where dQ denotes a normalized measure on the two sphere and the action is given by Eq. (35). Hence the edge theory defined by the action in Eq. (7), is exactly equivalent to a spin- $\frac{m}{2}$ system with the Hamiltonian given by (39). The correlation functions of the Q fields can be expressed in the operator formalism as,

$$\begin{aligned} s^n \langle Q_{p_1 p'_1}(x_1) \dots Q_{p_n p'_n}(x_n) \rangle &= \text{tr} \left(e^{-LH} \mathcal{T}_x (J_{p_1 p'_1}(x_1) \dots \right. \\ &\quad \left. \dots J_{p_n p'_n}(x_n)) \right), \end{aligned} \quad (42)$$

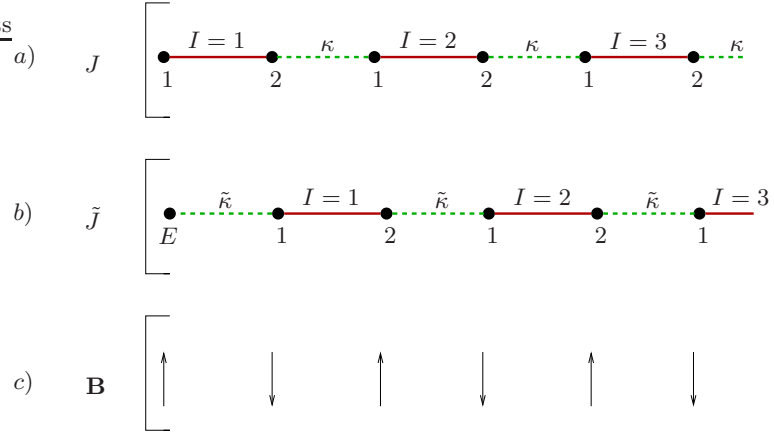


FIG. 3: Semi-infinite dimerized spin chain with no edge spin (a) and with the edge spin in the dual representation (b). The orientation of the staggered magnetic field is shown in (c).

where $J_{pp'} \equiv J^a \tau_{pp'}^a$. The (euclidean) equations of motion are easily solved,

$$J^3(x) = J^3(0) \quad (43)$$

$$J^+(x) = J^+(0) e^{\frac{\omega}{v_d} x} \quad (44)$$

$$J^-(x) = J^-(0) e^{-\frac{\omega}{v_d} x} \quad (45)$$

The only non-zero two point function at $L = \infty$ is easily computed to be,

$$\langle Q^{-+}(x_1) Q^{+-}(x_2) \rangle = m\theta(x_1 - x_2) e^{-2\frac{\omega}{v_d}(x_1 - x_2)} \quad (46)$$

which is exactly the result in Eq.(14). Thus we have shown that the critical edge action and correlation functions obtained in the bare strong coupling limit is exactly the same as that of a single spin- $\frac{m}{2}$ system for $N = M = 1$. These results can be generalized for all N and M . We will be presenting the results in a forthcoming publication.

III. DIMERIZED SPIN CHAINS

The results of the previous Section implies that the bare strong coupling limit of the NLSM is exactly equivalent to the low energy physics of spin- $\frac{m}{2}$ dimerized spin chain (DSC), in the strong dimerization limit. We first consider the case of semi-infinite DSC's and will discuss the case of finite chains later. The Hamiltonian is,

$$H_{DSC} = \sum_{I=0}^{\infty} J (\mathbf{S}_{2i} \cdot \mathbf{S}_{2i+1} + \kappa \mathbf{S}_{2i+1} \cdot \mathbf{S}_{2i+2}). \quad (47)$$

At $\kappa = 0$, the model consists of decoupled dimers and is trivially solved. All dimers being in the singlet state constitutes the ground state. Any one of the dimers being in the triplet state constitute the lowest energy excitations. Thus the system has a gap equal to J and there are no excitations at energy scales small compared to J .

At $\kappa = \infty$ also, the model decouples. The Hamiltonian can be written in a *dual* representation where the roles of the 'dimers' and the 'weak bonds' get interchanged (see Fig. 3),

$$\tilde{H}_{DSC} = \sum_{i=0}^{\infty} \tilde{J} (\tilde{\kappa} \mathbf{S}_{2i} \cdot \mathbf{S}_{2i+1} + \mathbf{S}_{2i+1} \cdot \mathbf{S}_{2i+2}). \quad (48)$$

where we have defined $\tilde{\kappa} \equiv \frac{1}{\kappa}$, $\tilde{J} \equiv \kappa J$. Thus $\kappa = \infty \Leftrightarrow \tilde{\kappa} = 0$. The system now decouples into a set of dimers and a free spin at the edge. The dynamics at energy scales small compared to J will therefore be that of the free spin at the edge (see Fig. 3b).

Thus, consistent with the Haldane mapping, the low energy physics of the DSC at $\kappa = 0$ and $\kappa = \infty$ is the same as that of the NLSM at $\sigma_{xx} = 0 = \sigma_{xy}$ and $\sigma_{xx} = 0$, $\sigma_{xy} = m$ respectively. In the former case both models have no low energy dynamics and in the latter case both have low energy dynamics confined to edge with identical correlation functions.

A. Haldane mapping with an edge

The above validation of the Haldane mapping in the strong coupling limit is of course somewhat trivial at this stage. We will later be developing formalism to justify the mapping at non-zero values of $\kappa(\tilde{\kappa})$. In this section we will perform the Haldane mapping, with the standard approximations, of the semi-infinite DSC to the NLSM with an edge. We point out some features and also discuss the approximations involved.

For $\kappa \leq 1$, it is useful to change the labeling of the spins and denote,

$$\begin{aligned}\mathbf{S}_{I,1} &\equiv \mathbf{S}_{2I}, \\ \mathbf{S}_{I,2} &\equiv \mathbf{S}_{2I+1}.\end{aligned}\tag{49}$$

The Hamiltonian is then written as,

$$H = J \left[\sum_{I=0}^{\infty} \mathbf{S}_{I,1} \cdot \mathbf{S}_{I,2} + \kappa \sum_{I=0}^{\infty} \mathbf{S}_{I,2} \cdot \mathbf{S}_{(I+1),1} \right].\tag{50}$$

For $\kappa \geq 1$, we denote,

$$\begin{aligned}\mathbf{S}_E &\equiv \mathbf{S}_0, \\ \mathbf{S}_{I,1} &\equiv \mathbf{S}_{2I+1}, \\ \mathbf{S}_{I,2} &\equiv \mathbf{S}_{2I+2}.\end{aligned}\tag{51}$$

The Hamiltonian in the dual representation is then,

$$\tilde{H} = \tilde{J} \left[\mathbf{S}_E \cdot \mathbf{S}_{0,1} + \tilde{\kappa} \sum_{I=0}^{\infty} \mathbf{S}_{I,1} \cdot \mathbf{S}_{I,2} + \sum_{I=0}^{\infty} \mathbf{S}_{I,2} \cdot \mathbf{S}_{I+1,1} \right].\tag{52}$$

The Hamiltonians H and \tilde{H} indicate that apart from edge effects the spin system has a *dual symmetry*

$$\begin{aligned}\kappa &\rightarrow \kappa^{-1}, \\ J &\rightarrow \kappa J.\end{aligned}\tag{53}$$

This symmetry has a different meaning dependent on the value s of the spin. In what follows we shall separately derive the effective action of the spin system in the completely equivalent representations given by H and \tilde{H} respectively.

To proceed it is helpful to introduce a staggered magnetic field \mathbf{B} in H .

$$H \rightarrow H + \sum_{I=0}^{\infty} \mathbf{B} \cdot (\mathbf{S}_{I,1} - \mathbf{S}_{I,2}).\tag{54}$$

This term favours an anti-ferromagnetic spin arrangement of the semi-infinite chain (see Fig. 1c). Notice that the same anti-ferromagnetic order is induced by adding the following terms to \tilde{H} .

$$\tilde{H} \rightarrow \tilde{H} + \mathbf{B}_0 \cdot \mathbf{S}_E - \sum_{I=0}^{\infty} \mathbf{B} \cdot (\mathbf{S}_{I,1} - \mathbf{S}_{I,2}).\tag{55}$$

Next it is convenient to introduce a slightly different notation for the dimer terms in the theory. Without loss of generality we may replace the terms $\mathbf{S}_{I,1} \cdot \mathbf{S}_{I,2}$ in H and \tilde{H} by the expression $\frac{1}{2}(\mathbf{S}_{I,1} + \mathbf{S}_{I,2})^2$. Keeping this in mind we obtain the euclidean action in the coherent state basis as follows.

$$S = is \sum_{I=0}^{\infty} \Omega[\hat{\mathbf{n}}_{I,1}] + \Omega[\hat{\mathbf{n}}_{I,2}] + s^2 J \int dt \sum_{I=0}^{\infty} \frac{1}{2} (\hat{\mathbf{n}}_{I,1} + \hat{\mathbf{n}}_{I,2})^2 + \kappa \hat{\mathbf{n}}_{I,2} \cdot \hat{\mathbf{n}}_{I+1,1} + s \int dt \sum_{I=0}^{\infty} \mathbf{B} \cdot (\hat{\mathbf{n}}_{I,1} - \hat{\mathbf{n}}_{I,2}),\tag{56}$$

where $\Omega[\hat{\mathbf{n}}]$ is the solid-angle subtended by $\hat{\mathbf{n}}$. This can be written as,

$$\Omega[\hat{\mathbf{n}}] = \int dt \int_0^1 du \hat{\mathbf{n}} \cdot \partial_t \mathbf{n} \times \partial_u \hat{\mathbf{n}}.\tag{57}$$

Here u is a fictitious dimension such that $\hat{\mathbf{n}}(u, t)|_{u=1} = \hat{\mathbf{n}}(t)$ and $\hat{\mathbf{n}}(u, t)|_{u=0} = \hat{\mathbf{z}}$.

Similarly we obtain in the dual representation,

$$\tilde{S} = \tilde{S}_{edge} + \tilde{S}_{bulk}, \quad (58)$$

where,

$$\tilde{S}_{edge} = is\Omega[\hat{\mathbf{n}}_E] + s^2\tilde{J} \int dt \tilde{\kappa} \hat{\mathbf{n}}_E \cdot \hat{\mathbf{n}}_{0,1} + s \int dt \mathbf{B}_0 \cdot \hat{\mathbf{n}}_E, \quad (59)$$

$$\begin{aligned} \tilde{S}_{bulk} = & is \sum_{I=0}^{\infty} \Omega[\hat{\mathbf{n}}_{I,1}] + \Omega[\hat{\mathbf{n}}_{I,2}] + s^2\tilde{J} \int dt \sum_{I=0}^{\infty} \frac{1}{2} (\hat{\mathbf{n}}_{I,1} + \hat{\mathbf{n}}_{I,2})^2 + \tilde{\kappa} \hat{\mathbf{n}}_{I,2} \cdot \hat{\mathbf{n}}_{I+1,1} \\ & - s \int dt \sum_{I=0}^{\infty} \mathbf{B} \cdot (\hat{\mathbf{n}}_{I,1} - \hat{\mathbf{n}}_{I,2}). \end{aligned} \quad (60)$$

B. Change of variables

Suppressing, for the time being, the index I then the new dimer field variables \mathbf{m} and \mathbf{l} are defined as follows

$$\mathbf{m} = \frac{(\hat{\mathbf{n}}_1 - \hat{\mathbf{n}}_2)}{2}, \quad (61)$$

$$\mathbf{l} = \frac{(\hat{\mathbf{n}}_1 + \hat{\mathbf{n}}_2)}{2}. \quad (62)$$

Here the variable \mathbf{m} describes the quantum fluctuations of the *anti-ferromagnetic* ordering whereas \mathbf{l} is associated with a *ferromagnetic* ordering of the spin chain. Since one expects the former to control the physics of the problem, the idea next is to eliminate the \mathbf{l} in a standard manner and formulate an effective action in terms of the field variable \mathbf{m} alone. It is easy to see that the effective theory only depends on the vector fields $\hat{\mathbf{m}}$ with unit length. To show this, notice that,

$$\begin{aligned} \hat{\mathbf{n}}_1^2 &= m^2 + l^2 + 2\mathbf{m} \cdot \mathbf{l} = 1, \\ \hat{\mathbf{n}}_2^2 &= m^2 + l^2 - 2\mathbf{m} \cdot \mathbf{l} = 1. \end{aligned} \quad (63)$$

Since we also have $\mathbf{m} \cdot \mathbf{l} = 0$, it follows that $m^2 = 1 - l^2$. Therefore, up to quadratic order in l , the vector fields $\hat{\mathbf{n}}_1, \hat{\mathbf{n}}_2$ can be written as,

$$\hat{\mathbf{n}}_1 = \left(1 - \frac{l^2}{2}\right) \hat{\mathbf{m}} + \mathbf{l}, \quad (64)$$

$$\hat{\mathbf{n}}_2 = -\left(1 - \frac{l^2}{2}\right) \hat{\mathbf{m}} + \mathbf{l}. \quad (65)$$

Using Eqs. (64) and (65) we now rewrite the terms in the action in terms of the new set of variables $\hat{\mathbf{m}}_I$ and \mathbf{l}_I . We proceed by presenting the final answer for S_{eff} , the intermediate steps can be found in Appendix A. This is obtained by integrating over the Gaussian fluctuations in the \mathbf{l} fields (which amounts to a systematic expansion of the theory in powers of $1/s$) and after taking the continuum limit. The result is,

$$S_{eff} = \int_0^\infty dx \int_0^\beta dt \mathcal{L}, \quad (66)$$

where,

$$\mathcal{L} = \frac{is\kappa}{(1+\kappa)} \hat{\mathbf{m}} \cdot \partial_t \hat{\mathbf{m}} \times \partial_x \hat{\mathbf{m}} + \frac{\kappa Js^2 a}{2(1+\kappa)} \partial_x \hat{\mathbf{m}} \cdot \partial_x \hat{\mathbf{m}} + \frac{1}{2(1+\kappa)Ja} \partial_t \hat{\mathbf{m}} \cdot \partial_t \hat{\mathbf{m}} - \frac{s}{a} \mathbf{B} \cdot \hat{\mathbf{m}}. \quad (67)$$

Here, $a/2$ is the lattice spacing. It is important to remark that the theory is defined with *free boundary conditions* on the vector field variables $\hat{\mathbf{m}}$. Notice that the presence of the staggered magnetic field (\mathbf{B}) term eliminates all the arbitrariness of the problem, indicating that S_{eff} is the appropriate quantum theory for anti-ferromagnetic ordering.

Next we compare the results with those obtained in the dual representation. In this case we obtain an extra piece associated with the edge vector field $\hat{\mathbf{n}}_E$. The answer can be written as,

$$\tilde{S}_{eff} = \tilde{S}_0 + \int_0^\infty dx \int_0^\beta dt \tilde{\mathcal{L}} \quad (68)$$

where,

$$\tilde{S}_0 = is \Omega[\hat{\mathbf{m}}(0, t)], \quad (69)$$

$$\tilde{\mathcal{L}} = -\frac{is\tilde{\kappa}}{(1+\tilde{\kappa})}\hat{\mathbf{m}} \cdot \partial_t \hat{\mathbf{m}} \times \partial_x \hat{\mathbf{m}} + \frac{\tilde{\kappa}\tilde{J}s^2a}{2(1+\tilde{\kappa})}\partial_x \hat{\mathbf{m}} \cdot \partial_x \hat{\mathbf{m}} + \frac{1}{2(1+\tilde{\kappa})\tilde{J}a}\partial_t \hat{\mathbf{m}} \cdot \partial_t \hat{\mathbf{m}} - \frac{s}{a}\mathbf{B} \cdot \hat{\mathbf{m}}, \quad (70)$$

and $\hat{\mathbf{m}}(0, t) = \hat{\mathbf{n}}_E(t)$.

C. Nonlinear sigma model

By rewriting the edge piece \tilde{S}_0

$$\tilde{S}_0 = is\Omega[\mathbf{m}(0)] = is \int dt \int dx \hat{\mathbf{m}} \cdot \partial_t \hat{\mathbf{m}} \times \partial_x \hat{\mathbf{m}} \quad (71)$$

we conclude that S_{eff} and the dual theory \tilde{S}_{eff} are identically the same. Thus we obtain the Lagrangian for the standard $O(3)$ nonlinear sigma model,

$$\mathcal{L}_{NLSM} = \frac{1}{2g} \left[c \partial_x \hat{\mathbf{m}} \cdot \partial_x \hat{\mathbf{m}} + \frac{1}{c} \partial_t \hat{\mathbf{m}} \cdot \partial_t \hat{\mathbf{m}} \right] + i \frac{\theta}{4\pi} \hat{\mathbf{m}} \cdot \partial_t \hat{\mathbf{m}} \times \partial_x \hat{\mathbf{m}} - \frac{s}{a} \mathbf{B} \cdot \hat{\mathbf{m}}. \quad (72)$$

We have introduced the spin-wave velocity c , the coupling constant g and the instanton angle θ which are expressed as follows,

$$c = as \sqrt{\tilde{\kappa}}J = as \sqrt{\tilde{\kappa}}\tilde{J}, \quad (73)$$

$$g = s^{-1} \frac{(1+\tilde{\kappa})}{\sqrt{\tilde{\kappa}}} = s^{-1} \frac{(1+\tilde{\kappa})}{\sqrt{\tilde{\kappa}}}, \quad (74)$$

$$\theta = 4\pi s \frac{\tilde{\kappa}}{1+\tilde{\kappa}} = 4\pi s \left[1 - \frac{\tilde{\kappa}}{1+\tilde{\kappa}} \right]. \quad (75)$$

D. Validity of the approximations

There are two standard approximations made in the Haldane mapping. First that \mathbf{l} is small and second that \mathbf{m} is a slowly varying field on the length scale of the lattice spacing. The small \mathbf{l} approximation (i.e retaining terms up to l^2) is basically a *kinematic* one that replaces the dimer by a rotor. For a single dimer, it results in an action

$$S = \int dt \frac{1}{2J} \partial_t \hat{\mathbf{m}} \cdot \partial_t \hat{\mathbf{m}}. \quad (76)$$

The Hilbert space of the rotor consists of one representation of each spin- j , $j = 0, 1, 2, \dots, \infty$ the spectrum being $E_j = \frac{1}{2J}j(j+1)$. The spin- s dimer has an identical Hilbert space and spectrum except that it is truncated at $j = 2s$. Thus the approximation becomes exact as $s \rightarrow \infty$. However, as we will argue, we may also expect it to be good at energy scales $E \leq J$, at small $\kappa(\tilde{\kappa})$. At $\kappa(\tilde{\kappa}) = 0$, the lowest excitations for both the decoupled rotor and the decoupled dimer system *at all* s , consist of one rotor(dimer) being excited to the triplet state. For weak coupling, the low energy physics of both the systems is that of weakly dispersing, weakly interacting triplets. Therefore even at $s = \frac{1}{2}$, we may expect the small \mathbf{l} approximation to be good for at small $\kappa(\tilde{\kappa})$ for energy scales $E \leq J$. The second approximation consist of taking the ‘naive’ continuum limit of the coupled rotor system which we call the *rotor chain* (RC). Namely assuming that the low energy physics is correctly described by slowly varying \mathbf{m} fields. This is clearly not valid for the physics of the triplets, since the \mathbf{m} fields are weakly coupled. However, if at energy scales $E \ll J$ the triplets are decoupled from the edge spin, then they are irrelevant to the physics at these scales. Thus if the system, under renormalization, flows to $\kappa = 0$, the naive continuum approximation will not affect the physics at energy scales small compared to the triplet gap.

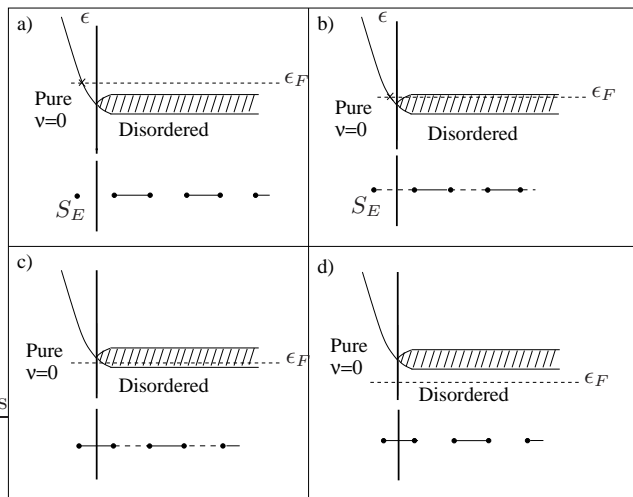


FIG. 4: Energy spectrum for a semi-infinite quantum Hall systems versus x and the corresponding dimerized spin chain. In (a) we sketch the situation of a fully occupied Landau band $\nu = 1$ (i.e. ϵ_F lies above the lowest Landau states) with massless excitations at the edge. The corresponding DSC consists of completely decoupled dimers ($\kappa = \infty$) with an isolated dangling spin at the edge, S_E . In (b) and (c) we sketch the situation where ϵ_F lies within the band such that $1 > \nu > 1/2$ (corresponding to the presence of weakly coupled edge spin) and $0 < \nu < 1/2$ (corresponding to the absence of a dangling edge spin) respectively. In situation (d) we have $\nu = 0$ (ϵ_F lies below the Landau band) and the corresponding DSC has completely decoupled dimers only ($\kappa = 0$).

IV. GEOMETRIES

In this Section we discuss the correspondence between quantum Hall systems of various different geometries and dimerized $s = \frac{1}{2}$ spin chains. This correspondence is established by comparing the parameters entering the effective nonlinear σ model action on the basis of which one expects that both systems display the same (super universal) features. The imaginary time t in the spin system translates into periodic boundary conditions the y direction (or a *cylinder geometry*) in the quantum Hall system. Furthermore, by considering a partially occupied lowest Landau band with a filling fraction $0 \leq \nu \leq 1$ then the correspondence is given by²

$$\sigma_{xx} \longleftrightarrow 1/2g = \frac{\sqrt{\kappa}}{1 + \kappa}, \quad (77)$$

$$\sigma_{xy} = \nu \longleftrightarrow \frac{\theta}{2\pi} = \frac{\kappa}{1 + \kappa}. \quad (78)$$

Here, σ_{xx} and σ_{xy} are the mean field values of the dimensionless *longitudinal* and *Hall* conductance respectively. Notice that a varying dimerization parameter κ in the DSC has the same meaning as a varying Fermi energy ϵ_F or filling fraction ν in the quantum Hall system. In what follows we shall represent the spin chain by an array of spins along the x axis and compare it with the disordered Landau level system at zero temperature that is depicted in the plane of energy versus the x axis.

A. Semi-infinite systems

In Fig. 4 we sketch the semi-infinite quantum Hall system with an edge at $x = 0$ and the corresponding DSC. The “edge states” in the quantum Hall system are represented by the center of the cyclotron orbits that formally lie outside the sample ($x < 0$). When the Fermi level (ϵ_F) lies above the lowest Landau band (Fig. 4a) then the bulk of the system is gapped but there are gapless excitations at the edge $x = 0$. In the effective non-linear σ model action the bare parameters σ_{xx} and $\sigma_{xy} = \nu$ are 0 and 1 respectively. According to Eqs. (72)-(75) this corresponds to a system of completely decoupled dimers with a dangling spin at the edge (S_E). Next, in Fig. 4b we consider the case where ϵ_F lies within the Landau band such that $1 > \nu > 1/2$. We now have $\sigma_{xx} > 0$ and $1/2 < \sigma_{xy} < 1$. The corresponding DSC has a weak bond at the edge (dashed line). Similarly, for $0 < \nu < 1/2$ (Fig. 4c) we have $\sigma_{xx} > 0$ and $0 < \sigma_{xy} < 1/2$ and the edge bond for the DSC is a strong one (bold line). Finally, in Fig. 4d we show the case

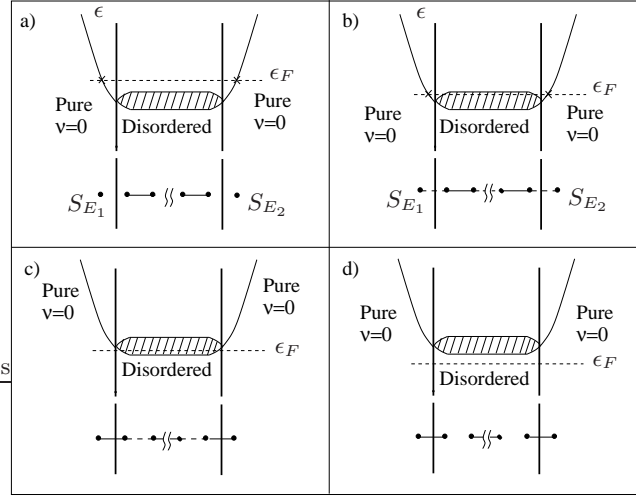


FIG. 5: Energy spectrum for Finite quantum Hall systems and correspondence with DSC's with an even number of sites. In (a) ϵ_F lies above the lowest Landau band and the DSC consisting of decoupled dimers has isolated spins at both the edges. In (b) and (c) ϵ_F is within the band with $\nu > 1/2$ (weakly coupled edge spins at both the edges) and $\nu < 1/2$ (no dangling edge spin) respectively. In (d) ϵ_F lies below the Landau band and the corresponding DSC has completely decoupled dimers with no isolated spins at the edges.

where ϵ_F lies below the Landau band or $\nu = 0$. In this case we have $\sigma_{xx} = \sigma_{xy} = 0$ and there are clearly no edge states. The corresponding DSC consists of completely decoupled dimers without a dangling spin at the edge.

B. Finite systems and DSC with even number of sites

A finite disordered sample has edges at $x = 0$ and $x = L$ respectively (Fig. 5). It is easy to see that the corresponding spin chain is finite as well but it must have an *even* number of sites. This is so because the quantum Hall system with a completely filled Landau band ($\nu = 1$, Fig. 5a) has massless excitations at both the edges. The corresponding DSC must therefore have dangling spins at both the edges and this only happens when the total number of sites is *even*. For $\nu = 0$ (Fig. 5d) there are no quantum Hall edge states and the corresponding spin chain has dimers at both the edges (bold lines), i.e. no dangling spins. The intermediate situations $1/2 < \nu < 1$ and $0 < \nu < 1/2$ are depicted in Figs. 5c and 5d respectively.

C. Finite systems and DSC with odd number of sites

Fig. 6 sketches the correspondence between a quantum Hall system and a finite spin chain with an *odd* number of sites. In this case the quantum Hall system defined for $0 < x < L$ is flanked on the right hand side ($x > L$) by the trivial vacuum or $\nu = 0$. On the left hand side ($x < 0$), however, the system is flanked by a semi-infinite quantum Hall state with a fixed filling fraction $\nu = 1$ such that in this region the Fermi level ϵ_F is always located above the Landau band. The effect of the $\nu = 1$ quantum Hall state for $x < 0$ on the energy of the massless edge excitations at $x = 0$ is indicated in Fig. 6. Notice that this system formally describes a semi-infinite quantum Hall system defined for $-\infty < x < L$ where, say, the value of the external magnetic field for $x < 0$ is different from that for $x > 0$. The Lagrangian for $0 < x < L$ has parameters σ_{xx} and σ_{xy} as in Eqs. (77) and (78). However, for $x < 0$ the action is not zero but, rather, the parameters σ_{xx} and σ_{xy} are now fixed and given by 0 and 1 respectively. It is readily verified that the quantum Hall system with varying values of ϵ_F or ν in the interval $0 < x < L$ displays the same basic features as the DSC with an *odd* number of sites and with varying values of the parameter κ , see Figs. 6 a-d. The Lagrangian in this case is defined by

$$\mathcal{L}_{NLSM} = \frac{i}{2} \hat{\mathbf{m}} \cdot \partial_t \hat{\mathbf{m}} \times \partial_x \hat{\mathbf{m}} \quad (x < 0) \quad (79)$$

$$= \frac{1}{2g} \left[c \partial_x \hat{\mathbf{m}} \cdot \partial_x \hat{\mathbf{m}} + \frac{1}{c} \partial_t \hat{\mathbf{m}} \cdot \partial_t \hat{\mathbf{m}} \right] + \frac{i\theta}{4\pi} \hat{\mathbf{m}} \cdot \partial_t \hat{\mathbf{m}} \times \partial_x \hat{\mathbf{m}} \quad (0 < x < L) \quad (80)$$

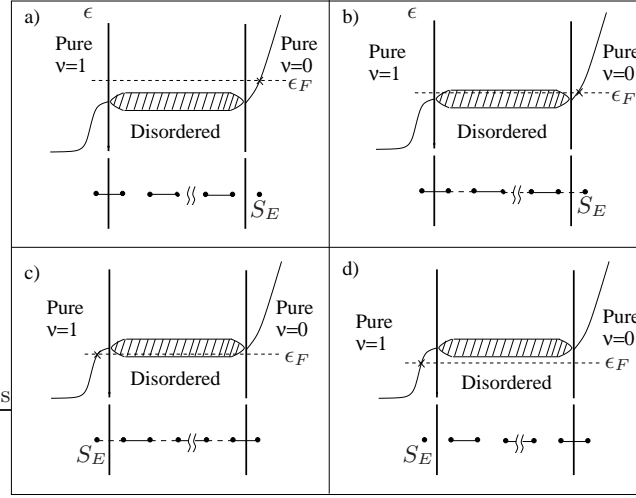


FIG. 6: Energy spectrum for a *semi infinite* quantum Hall system with a fixed filling fractions $\nu = 1$ for $x < 0$ and $\nu = 0$ for $x > L$. The corresponding DSC is *finite* with an *odd* number of sites in the interval $0 < x < L$. In situation (a) the Fermi energy ϵ_F lies above the lowest Landau band and the corresponding DSC consists of decoupled dimers with an dangling edge spin on the right. In (b) and (c) ϵ_F lies within the band with $\nu > 1/2$ (corresponding to a weakly coupled edge spin on the right) and $\nu < 1/2$ (corresponding to a weakly coupled edge spin on the left) respectively. In (d) we show the case where ϵ_F lies below the Landau band. The corresponding DSC has completely decoupled dimers with a dangling spin at the left edge.

V. THE REAL SPACE RENORMALIZATION GROUP SCHEME

We now formulate a real space renormalization group scheme using a combination of Hamiltonian and path integral techniques. The scheme involves a systematic perturbative expansion in the weak inter-dimer coupling and in time derivatives. We compute the RG equations to lowest non-trivial order in both the coupling and in derivatives and discuss the solutions.

A. The decimation scheme

We begin with the path integral representation of the DSC,

$$Z = \text{tr} e^{-\beta H} = \int \prod_{I\alpha} \mathcal{D}[\hat{\mathbf{n}}_{I\alpha}] e^{-S[\{\hat{\mathbf{n}}_{I\alpha}\}]}, \quad (81)$$

where the action is given in Eq. (67). The decimation scheme consists of integrating out half the dimers (say the odd ones) in the path integral in Eq. (81) to obtain an effective action for the even dimers,

$$S^{eff} = \sum_{I\alpha} -\frac{i}{2} \Omega [\hat{\mathbf{n}}_{2I\alpha}] + \frac{1}{4} \int_{-\infty}^{\infty} d\tau \sum_I (\hat{\mathbf{n}}_{I1} \cdot \hat{\mathbf{n}}_{I2}) + S_{int}^{eff}, \quad (82)$$

where S_{int}^{eff} is given by,

$$\begin{aligned} e^{-S_{int}^{eff}} &= \int \prod_{I\alpha} \mathcal{D}[\hat{\mathbf{n}}_{(2I+1),\alpha}] \exp \left(- \sum_{I\alpha} -\frac{i}{2} \Omega [\hat{\mathbf{n}}_{(2I+1),\alpha}] \right) \\ &\times \exp \left(-\frac{1}{4} \int_{-\infty}^{\infty} d\tau \sum_I \hat{\mathbf{n}}_{(2I+1),1} \cdot \hat{\mathbf{n}}_{(2I+1),2} \right) \\ &\times \exp \left(-\frac{1}{4} \int_{-\infty}^{\infty} d\tau \sum_I \kappa [\hat{\mathbf{n}}_{(2I,2)} \cdot \hat{\mathbf{n}}_{(2I+1),1} + \hat{\mathbf{n}}_{(2I+1),2} \cdot \hat{\mathbf{n}}_{(2I+2),1}] \right), \\ e^{-S_{int}^{eff}} &= \prod_I \int \mathcal{D}[\hat{\mathbf{n}}_1] \mathcal{D}[\hat{\mathbf{n}}_2] \exp \left(\frac{i}{2} \sum_{\alpha} \Omega [\hat{\mathbf{n}}_{\alpha}] \right) \exp \left(-\frac{1}{4} \int_{-\infty}^{\infty} d\tau (\hat{\mathbf{n}}_1 \cdot \hat{\mathbf{n}}_2 + \kappa [\hat{\mathbf{n}}_2 \cdot \hat{\mathbf{n}}_{(2I+2),1} + \hat{\mathbf{n}}_1 \cdot \hat{\mathbf{n}}_{2I,2}]) \right). \quad (83) \end{aligned}$$

Therefore, computing S_{int}^{eff} involves computing the partition function of a two-spin system in the presence of time dependent external fields. This two-spin problem can be expressed in the Hamiltonian formalism as,

$$e^{-F[\mathbf{m}_1, \mathbf{m}_2]} = \text{tr} \left(T \exp \left[- \int_{-\infty}^{\infty} d\tau (h_0 + \kappa h_{int}) \right] \right), \quad (84)$$

where,

$$h_0 = \frac{1}{2}(\mathbf{S}_1 + \mathbf{S}_2)^2, \quad (85)$$

$$h_{int} = \mathbf{S}_1 \cdot \mathbf{m}_2(\tau) + \mathbf{S}_2 \cdot \mathbf{m}_1(\tau). \quad (86)$$

Here we have defined,

$$\mathbf{m}_1 = \frac{1}{2} \hat{\mathbf{n}}_{(I-1),1}, \quad \mathbf{m}_2 = \frac{1}{2} \hat{\mathbf{n}}_{(I+1),2}. \quad (87)$$

B. The renormalization group equations

F can be expanded systematically in a cumulant expansion in powers of κ . To order $\sim \kappa^2$,

$$F = -\frac{\kappa^2}{2!} \int_{-\infty}^{\infty} d\tau_1 d\tau_2 \langle 0 | T(h_{int}(\tau_1) h_{int}(\tau_2)) | 0 \rangle. \quad (88)$$

This is computed to be,

$$F = -\frac{\kappa^2}{4} \int_{-\infty}^{\infty} d\tau \int_0^{\infty} dt e^{-t} m^a(\tau + t/2) m^a(\tau - t/2), \quad (89)$$

where $\mathbf{m} = \mathbf{m}_1 - \mathbf{m}_2$. For fields slowly varying over a time scale of ~ 1 , we can expand $m^a(\tau \pm t)$ about τ and develop a local derivative expansion for F . For the moment we neglect the derivatives and get,

$$F = -\frac{\kappa^2}{8} \int_{-\infty}^{\infty} d\tau \mathbf{m}_1 \cdot \mathbf{m}_2. \quad (90)$$

Using Eqs. (82,83,87,90) and relabeling the sites $2I \rightarrow I$, we get the effective Hamiltonian,

$$H_{eff} = \sum_I (\mathbf{S}_{I1} \cdot \mathbf{S}_{I2} + \kappa' \mathbf{S}_{I2} \cdot \mathbf{S}_{I+11}). \quad (91)$$

This is exactly of the initial form in Eq. (47), with the renormalized coupling $\kappa' = \kappa^2/2$. We therefore have the recursion relation for the coupling constant,

$$\kappa^{n+1} = \frac{(\kappa^n)^2}{2}. \quad (92)$$

The solution to this recurrence relation is,

$$\kappa^n = 2 \left(\frac{\kappa^0}{2} \right)^L, \quad L \equiv 2^n. \quad (93)$$

Thus, there are two fixed points,

$$\kappa^* = 0 \quad \text{and} \quad \kappa^* = 2, \quad (94)$$

and the coupling constant flows from $\kappa^* = 2$ to $\kappa^* = 0$. Note that the Hamiltonian in Eq. (47) with coupling $\kappa = 1$, the $s = 1/2$ uniform Heisenberg chain, is known to be gap-less. This implies that $\kappa^* = 1$, corresponding to $\theta = \pi$ has to be a fixed point of the RG equations. As we will see in the next section, this error is due to the neglecting of the time derivatives.

C. Time derivatives

The RHS of Eq. (89) can be expanded to second order in the derivatives and the effective action computed. We obtain,

$$S^{eff} = \int_{-\infty}^{\infty} d\tau \left(\sum_{I\alpha} -\frac{i}{2} \mathbf{A}_{mon}(\hat{\mathbf{n}}_{I\alpha}) \cdot \partial_\tau \hat{\mathbf{n}}_{I\alpha} + \frac{\kappa'}{8} \partial_\tau \hat{\mathbf{n}}_{I\alpha} \cdot \partial_\tau \hat{\mathbf{n}}_{I\alpha} + \sum_I \frac{1}{8} \hat{\mathbf{n}}_{I1} \cdot \hat{\mathbf{n}}_{I2} + \frac{\kappa'}{4} [\hat{\mathbf{n}}_{I2} \cdot (1 + \partial_\tau^2) \hat{\mathbf{n}}_{I+12}] \right).$$

The system described by the above action is no longer a spin chain. It now corresponds to a system of charged particles confined to the surface of a sphere with a unit monopole at the center. If we neglect the derivative terms coupling neighbouring sites, the Hilbert space at each site has one representation of all half odd integer angular momenta, $J = 1/2, 3/2, 5/2, \dots$. Namely, at every site we have a fermionic rotor. Thus under renormalization, the spin chain goes over to a fermionic rotor chain (FRC). This can be understood qualitatively as follows. The degree of freedom at each site in the effective action corresponds to the motion of the original spin at that site and a block of even number of spins that have been integrated out. Thus we can expect many excitations with higher (half odd integer) angular momenta.

D. The fermionic rotor chain

We therefore begin with a general FRC described by the action,

$$S = \int_{-\infty}^{\infty} d\tau \left[\sum_{I\alpha} \left(-\frac{i}{2} \mathbf{A}_{mon}(\hat{\xi}_{I\alpha}) \cdot \partial_\tau \hat{\xi}_{I\alpha} + \frac{\kappa_3 s'^2}{2} \partial_\tau \hat{\xi}_{I\alpha} \cdot \partial_\tau \hat{\xi}_{I\alpha} \right) + \sum_I s'^2 \left(\kappa_4 \hat{\xi}_{I1} \cdot \partial_\tau^2 \hat{\xi}_{I2} + \kappa_2 \hat{\xi}_{I2} \cdot \partial_\tau^2 \hat{\xi}_{(I+1),1} \right) + \sum_I s'^2 \left(\hat{\xi}_{I1} \cdot \hat{\xi}_{I2} + \kappa_1 \hat{\xi}_{I2} \cdot \hat{\xi}_{(I+1),1} \right) \right]. \quad (95)$$

We have introduced four coupling constants, $\kappa_1, \kappa_2, \kappa_3$ and κ_4 . $s' \equiv 3/2$ for reasons that will become clear later. A model of this type for a uniform chain has been previously considered in reference¹⁴. Our dimerized model has the duality of the DSC. If we make the transformation,

$$\hat{\xi}_{I1} \rightarrow \hat{\xi}_{I2}, \quad \hat{\xi}_{I2} \rightarrow \hat{\xi}_{(I+1),1} \quad \text{and} \quad \tau \rightarrow \frac{\tau}{\kappa_1}, \quad (96)$$

we get back exactly the same model with $\kappa_i \rightarrow \tilde{\kappa}_i$, where,

$$\tilde{\kappa}_1 = \frac{1}{\kappa_1}, \quad \tilde{\kappa}_2 = \kappa_4 \kappa_1, \quad \tilde{\kappa}_3 = \kappa_3 \kappa_1 \quad \text{and} \quad \tilde{\kappa}_4 = \kappa_2 \kappa_1. \quad (97)$$

The action for the dimer problem is now,

$$S = \int_{-\infty}^{\infty} d\tau \left[\sum_\alpha \left(-\frac{i}{2} \mathbf{A}_{mon}(\hat{\xi}_\alpha) \cdot \partial_\tau \hat{\xi}_\alpha + \frac{\kappa_3 s'^2}{2} \partial_\tau \hat{\xi}_\alpha \cdot \partial_\tau \hat{\xi}_\alpha + s'^2 \hat{\xi}_\alpha \cdot \mathbf{m}_\alpha \right) + \kappa_4 s'^2 \hat{\xi}_{I1} \cdot \partial_\tau^2 \hat{\xi}_{I2} + s'^2 \hat{\xi}_1 \cdot \hat{\xi}_2 \right], \quad (98)$$

where,

$$\mathbf{m}_1 = (\kappa_1 + \kappa_2 \partial_\tau^2) \hat{\xi}_{(I-1),2}, \quad (99)$$

$$\mathbf{m}_2 = (\kappa_1 + \kappa_2 \partial_\tau^2) \hat{\xi}_{(I+1),1}. \quad (100)$$

We first put $\kappa_4 = 0$ and discuss the effects of it being non-zero later. The Hamiltonian corresponding to the action in Eq. (98) is then,

$$h_d = h_0 + h_{int}, \quad (101)$$

$$h_0 = \frac{1}{2\kappa_3 s'^2} \sum_\alpha (\mathbf{J}_\alpha \cdot \mathbf{J}_\alpha - \frac{1}{4}), \quad (102)$$

$$h_{int} = s'^2 \hat{\xi}_1 \cdot \hat{\xi}_2 + s' \sum_\alpha \hat{\xi}_\alpha \cdot \mathbf{m}_\alpha. \quad (103)$$

\mathbf{J}_α are the angular momentum operators. The spectrum of h_0 is,

$$h_0|(j_1, m_1), (j_2, m_2)\rangle = E_{j_1, j_2}|(j_1, m_1), (j_2, m_2)\rangle, \quad (104)$$

$$E_{j_1, j_2} = \frac{1}{2\kappa_3 s'^2} \sum_\alpha \left(j_\alpha(j_\alpha + 1) - \frac{1}{4} \right),$$

with $j_\alpha = 1/2, 3/2, \dots$ and $m_\alpha = -j_\alpha \dots j_\alpha$. The ground states are the four $j_1 = j_2 = 1/2$ states. When $\kappa_3 \ll 1$, the gap between the $(1/2, 1/2)$ states and the excited states is very large. In this limit, to a very good approximation, we can project the model into the $(j_1, j_2) = (1/2, 1/2)$ subspace. The matrix elements of $\hat{\mathbf{n}}$ between the $j = 1/2$ states can be explicitly computed using the monopole harmonics and we have,

$$\langle \frac{1}{2}, \sigma_1 | n^a | \frac{1}{2}, \sigma_2 \rangle = \frac{2}{3} S^a = \frac{1}{s'} S^a. \quad (105)$$

Thus to leading order in κ_3 , we recover the two-spin system as the effective Hamiltonian,

$$h_{eff} = \mathbf{S}_1 \cdot \mathbf{S}_2 + \sum_\alpha \mathbf{S}_\alpha \cdot \mathbf{m}_\alpha.$$

The previous results can now be used to integrate out the dimer system and get the recursion relations to second order in the κ 's. They are,

$$\kappa_1^{(n+1)} = \frac{\left(\kappa_1^{(n)} \right)^2}{2}, \quad (106)$$

$$\kappa_2^{(n+1)} = \frac{\left(\kappa_1^{(n)} \right)^2}{2} + \kappa_1^n \kappa_2^n, \quad (107)$$

$$\kappa_3^{(n+1)} = \kappa_3^n + \frac{\left(\kappa_1^{(n)} \right)^2}{2} + \kappa_1^n \kappa_2^n. \quad (108)$$

E. The strong coupling fixed points

The recursion relations in Eqs. (106), (107) and (108) can be solved explicitly with the initial conditions,

$$\kappa_1^{(0)} = \kappa_{10}, \quad \kappa_2^{(0)} = \kappa_{20}, \quad \kappa_3^{(0)} = \kappa_{30}. \quad (109)$$

The solution is,

$$\kappa_1^{(n)} = 2 \left(\frac{\kappa_{10}}{2} \right)^L, \quad (110)$$

$$\kappa_2^{(n)} = (aL - 1) \kappa_1^{(n)}, \quad (111)$$

$$\kappa_3^{(n)} = \kappa_{30} + \sum_{m=0}^{n-1} \kappa_2^{(m)}. \quad (112)$$

Where $L \equiv 2^n$ as before and $a = (1 + \kappa_{10}/\kappa_{20})$. These recursion relations have an infrared stable coupling fixed point which can be written as,

$$\kappa_1 = 0, \quad \kappa_2 = 0, \quad \kappa_3 = \kappa_3^* \neq \kappa_{30}. \quad (113)$$

As will be discussed in more detail below, the above fixed point is obtained provided the initial condition $\kappa_{10} < 2$ is satisfied. Notice that when $\kappa_{10} = 2$ we have $\kappa_1^n = 2$ but the value of κ_2^n diverges for large n and so does $\kappa_3^{(n)}$ as well as κ_3^* . Thus while the intermediate coupling fixed point, $\kappa_1^* = 2$ obtained earlier remains a fixed point of Eq. (106), the value of the new parameters lie outside the range of validity of the recursion relations, $\kappa_2^* = \kappa_3^* = \infty$. In particular, the decimation procedure has been evaluated under the assumption $\kappa_3 \ll 1$ which is clearly violated by the intermediate coupling fixed point with $\kappa_1^* = 2$. In what follows we shall study the validity of our renormalization

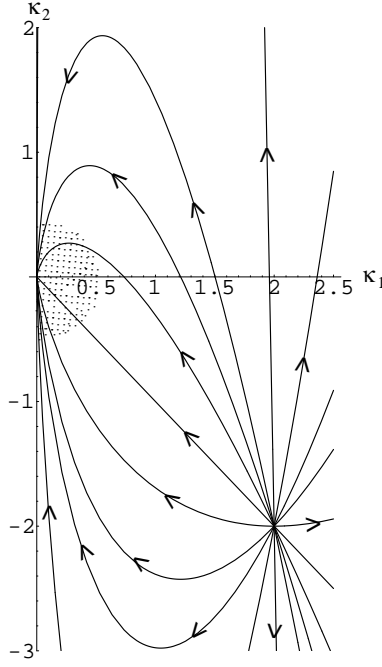


FIG. 7: Renormalization group flow in the κ_1 - κ_2 plane.

procedure in more detail. More specifically, we are interested in finding a subset of the parameter space $(\kappa_1, \kappa_2, \kappa_3)$ that satisfies $\kappa_3^{(n)} \ll 1$ for all positive integer values of n .

To start we write the recursion relations in differential form. From Eq. (110) and (111) we immediately obtain the following renormalization group equations,

$$\beta_1(\kappa_1) = \frac{d\kappa_1}{d\ln L} = \kappa_1 \ln \kappa_1/2, \quad (114)$$

$$\beta_2(\kappa_1, \kappa_2) = \frac{d\kappa_2}{d\ln L} = \kappa_1 + \kappa_2 + \kappa_2 \ln \kappa_1/2. \quad (115)$$

The various different renormalization group trajectories in the (κ_1, κ_2) plane can be found by solving the differential equation,

$$\frac{d\kappa_2}{d\kappa_1} = \beta_2(\kappa_1, \kappa_2)/\beta_1(\kappa_1). \quad (116)$$

The various solutions to Eqs. (114) - (116) are sketched in Fig. 7. This clearly indicates that the fixed point $(\kappa_1, \kappa_2) = (0, 0)$ is a completely *stable* in the *infrared*. On the other hand, a *finite* intermediate fixed point does exist at $(\kappa_1, \kappa_2) = (2, -2)$ but it is completely *unstable*.

The main issue next is to obtain an explicit expression for the quantity κ_3^* in Eq. (113). Let $(\kappa_1^{(n)}, \kappa_2^{(n)})$ denote a point close to the strong coupling fixed point $(0, 0)$. It is then possible to find a function F ,

$$\kappa_3^{(n)} = F(\kappa_1^{(n)}, \kappa_2^{(n)}), \quad (117)$$

that is the solution of the recursion relation of Eq. (108). To lowest order in the quantities $\kappa_1^{(n)}, \kappa_2^{(n)}$ we obtain,

$$F(\kappa_1^{(n)}, \kappa_2^{(n)}) = \kappa_3^* - \frac{(\kappa_1^{(n)})^2}{2} - \kappa_1^{(n)} \kappa_2^{(n)} + \mathcal{O}\left((\kappa^{(n)})^4\right). \quad (118)$$

On the basis of this result we obtain the following expressions for $\kappa_3^{(n)}$ with $n = 0$ and $n \rightarrow \infty$ respectively,

$$\kappa_3^{(0)} = \kappa_3^* - \frac{(\kappa_1^{(0)})^2}{2} - \kappa_1^{(0)} \kappa_2^{(0)} + \mathcal{O}\left((\kappa^{(0)})^4\right), \quad (119)$$

$$\kappa_3^{(n)} \rightarrow \kappa_3^* + \mathcal{O}\left(e^{-2L/\xi}\right). \quad (120)$$

The first of these equations expresses κ_3^* in terms of the renormalization points $\kappa^{(0)}$.

$$\kappa_3^* = \kappa_3^{(0)} + \frac{(\kappa_1^{(0)})^2}{2} + \kappa_1^{(0)} \kappa_2^{(0)} + \mathcal{O}\left((\kappa^{(0)})^4\right). \quad (121)$$

Eq. (120), on the other hand, tells us that the quantity κ_3^* appearing in Eqs. (121) and (113) are indeed identically the same. The final result of Eq. (121) can be used to identify the set of points $\{\kappa_1^{(0)}, \kappa_2^{(0)}\}$ in the κ_1, κ_2 plane for which the conditions,

$$0 \leq \kappa_3^{(0)} \ll 1, \quad 0 \leq \kappa_3^* \ll 1, \quad (122)$$

can be satisfied simultaneously. This set is indicated by the shaded area in Fig. 7.

We will now discuss the effects of turning on κ_4 . The first point to note is that κ_4 does not renormalize. This is because in the action in Eq. (95) the I^{th} dimer couples to $\hat{\xi}_{I+1,2}$ and $\hat{\xi}_{I-1,1}$. Thus, in the absence of next nearest neighbor couplings, integrating out the I^{th} dimer cannot produce a coupling between the two $\hat{\xi}$'s on the same dimer.

The κ_4 term breaks the $SU(2) \times SU(2)$ of the dimer Hamiltonian h_0 in Eq. (102). For small κ_4 , the low energy subspace will remain the $(j_1, j_2) = (1/2, 1/2)$ subspace. Then the two-spin effective Hamiltonian has to be of the form,

$$h_{eff} = (1 + \gamma(\kappa_4)) \mathbf{S}_1 \cdot \mathbf{S}_2 + \sum_{\alpha} \mathbf{S}_{\alpha} \cdot \mathbf{m}_{\alpha}, \quad (123)$$

where $\gamma(0) = 0$. A non-zero γ does not change the RG flow discussed above qualitatively. Its main effect is just to change the value of the intermediate coupling fixed point. However, as we discussed earlier, our current leading order calculation is not expected to be accurate in that regime. Thus κ_4 does not effect the strong coupling fixed point significantly and we will not discuss its effect in any more detail at this stage.

VI. HALDANE MAPPING FOR THE FERMIONIC ROTOR CHAIN

We will now examine the FRC in some detail. The low energy physics of the FRC can be mapped on to the NLSM similar to the Haldane mapping of the DSC to the NLSM. Consider the FRC defined in Eq. (95). As we did previously, define,

$$\mathbf{m} = \frac{\hat{\xi}_1 - \hat{\xi}_2}{2} \quad \text{and} \quad \boldsymbol{\lambda} = \frac{\hat{\xi}_1 + \hat{\xi}_2}{2}. \quad (124)$$

They satisfy the following constraints,

$$m^2 + \lambda^2 = 1 \quad \text{and} \quad \mathbf{m} \cdot \boldsymbol{\lambda} = 0. \quad (125)$$

We now express the different terms in the action in terms of the dimer variables \mathbf{m} and $\boldsymbol{\lambda}$ defined in Eqs. (124). Then,

$$-\frac{i}{2} \sum_{\alpha} \mathbf{A}_{mon}(\hat{\xi}_{I\alpha}) = -i \boldsymbol{\lambda}_I \cdot \hat{\mathbf{m}}_I \times \partial_{\tau} \hat{\mathbf{m}}_I. \quad (126)$$

This is an exact expression¹⁵. It is not possible to write the sum of the two solid angle terms as a local τ integral because the coordinate $\hat{\mathbf{m}}$ is singular when $\vec{\lambda} = 0$. However these points correspond to the two fermionic rotors in the dimer being aligned parallel and are hence not important configurations. The rest of the terms are expanded to quadratic order in $|\boldsymbol{\lambda}_I|$. Then,

$$S = \int_{-\infty}^{\infty} d\tau \left(s'^2 (\kappa_2 + \kappa_3 + \kappa_4) \partial_{\tau} \hat{\mathbf{m}}_I \cdot \partial_{\tau} \hat{\mathbf{m}}_I - \kappa_1 s'^2 \hat{\mathbf{m}}_I \cdot \hat{\mathbf{m}}_{(I+1)} \right) + S_{\lambda}, \quad (127)$$

$$S_{\lambda} = \int_{-\infty}^{\infty} d\tau \left(\boldsymbol{\lambda}_I \cdot \mathcal{A}_{IJ} \boldsymbol{\lambda}_J + \boldsymbol{\lambda}_I \cdot \vec{\mathcal{B}}_I \right) \quad (128)$$

$$\begin{aligned} \mathcal{A}_{IJ} \equiv & \left(2s'^2 - s'^2 (\kappa_3 - \kappa_2 - \kappa_4) \partial_{\tau}^2 \right) \delta_{IJ} + \kappa_1 s'^2 \delta_{(I+1)J} \\ & + \left(\kappa_1 s'^2 \hat{\mathbf{m}}_I \cdot \hat{\mathbf{m}}_{(I+1)} + s'^2 (\kappa_2 + \kappa_3 + \kappa_4) \partial_{\tau} \hat{\mathbf{m}}_I \cdot \partial_{\tau} \hat{\mathbf{m}}_I \right) \delta_{IJ} \end{aligned} \quad (129)$$

$$\vec{\mathcal{B}}_I \equiv \kappa_1 s'^2 (\hat{\mathbf{m}}_{(I+1)} - \hat{\mathbf{m}}_{(I-1)}) - i \hat{\mathbf{m}}_I \times \partial_{\tau} \hat{\mathbf{m}}_I$$

A. The continuum limit

We now take the continuum limit as follows. The continuum fields, $\hat{\mathbf{m}}(\tau, x)$ and $\boldsymbol{\lambda}(\tau, x)$ are defined as,

$$\hat{\mathbf{m}}(\tau, aI) \equiv \hat{\mathbf{m}}_I(\tau), \quad (130)$$

$$\boldsymbol{\lambda}(\tau, aI) \equiv \boldsymbol{\lambda}_I(\tau), \quad (131)$$

where a is the lattice spacing. We now assume that the fields $\hat{\mathbf{m}}(\tau, x)$ and $\boldsymbol{\lambda}(\tau, x)$ vary slowly over a length scale of a and a time scale of 1, and hence drop all derivatives of order greater than two. Then we have,

$$\begin{aligned} S &= \int_{-\infty}^{\infty} d\tau dx \left(\frac{\mathcal{I}}{2} \partial_{\tau} \hat{\mathbf{m}} \cdot \partial_{\tau} \hat{\mathbf{m}} + \frac{a\kappa_1 s'^2}{2} \partial_x \hat{\mathbf{m}} \cdot \partial_x \hat{\mathbf{m}} \right) + S_{\lambda}, \\ S_{\lambda} &= \int_{-\infty}^{\infty} d\tau dx \left[\frac{\mu}{2} \partial_{\tau} \boldsymbol{\lambda} \cdot \partial_{\tau} \boldsymbol{\lambda} - \frac{\kappa_1 s'^2 a}{2} \partial_x \boldsymbol{\lambda} \cdot \partial_x \boldsymbol{\lambda} \right. \\ &\quad + \left(\frac{2s'^2(1+\kappa_1)}{a} + \frac{\mathcal{I}}{2} \partial_{\tau} \hat{\mathbf{m}} \cdot \partial_{\tau} \hat{\mathbf{m}} - \frac{\kappa_1 s'^2 a}{2} \partial_x \hat{\mathbf{m}} \cdot \partial_x \hat{\mathbf{m}} \right) \boldsymbol{\lambda} \cdot \boldsymbol{\lambda} \\ &\quad \left. + \left(2\kappa_1 s'^2 \partial_x \hat{\mathbf{m}} - \frac{i}{a} \hat{\mathbf{m}} \times \partial_{\tau} \hat{\mathbf{m}} \right) \cdot \boldsymbol{\lambda} \right], \end{aligned} \quad (132)$$

where $\mathcal{I} \equiv (2s'^2/a)(\kappa_2 + \kappa_3 + \kappa_4)$ and $\mu \equiv (2s'^2/a)(\kappa_3 - \kappa_2 - \kappa_4)$. We now do the rescaling $\boldsymbol{\lambda} \rightarrow \sqrt{a}\boldsymbol{\lambda}$, and drop terms of $\mathcal{O}(a)$. Then we have,

$$S_{\lambda} = \int_{-\infty}^{\infty} d\tau dx \left[2s'^2(1+\kappa_1) \boldsymbol{\lambda} \cdot \boldsymbol{\lambda} + \left(2\kappa_1 s'^2 \partial_x \hat{\mathbf{m}} - \frac{i}{a} \hat{\mathbf{m}} \times \partial_{\tau} \hat{\mathbf{m}} \right) \cdot \sqrt{a}\boldsymbol{\lambda} \right]. \quad (133)$$

Integrating out $\boldsymbol{\lambda}$ we obtain the effective NLSM.

$$S_{NLSM} = \int d\tau dx \left(\frac{\tilde{\mathcal{I}}}{2} \partial_{\tau} \hat{\mathbf{m}} \cdot \partial_{\tau} \hat{\mathbf{m}} + \frac{\gamma}{2} \partial_x \hat{\mathbf{m}} \cdot \partial_x \hat{\mathbf{m}} + \frac{i\theta}{4\pi} \hat{\mathbf{m}} \cdot \partial_x \hat{\mathbf{m}} \times \partial_{\tau} \hat{\mathbf{m}} \right), \quad (134)$$

where the moment of inertia $\tilde{\mathcal{I}}$, the stiffness constant γ and the instanton angle θ are given by,

$$\tilde{\mathcal{I}} = \left(\mathcal{I} + \frac{1}{4s'^2 a(1+\kappa_1)} \right), \quad (135)$$

$$\gamma = \frac{a\kappa_1 s'^2}{(1+\kappa_1)}, \quad (136)$$

$$\theta = 2\pi \frac{\kappa_1}{(1+\kappa_1)}. \quad (137)$$

The coupling constant g and spin wave velocity c are then,

$$\frac{1}{g} = \left(\frac{\kappa_1(8s'^4(1+\kappa_1)(\kappa_2 + \kappa_3 + \kappa_4) + 1)}{4(1+\kappa_1)^2} \right)^{\frac{1}{2}}, \quad (138)$$

$$c = \left(\frac{4a^2 \kappa_1 s'^4}{8s'^4(1+\kappa_1)(\kappa_2 + \kappa_3 + \kappa_4) + 1} \right)^{\frac{1}{2}}. \quad (139)$$

B. The weak coupling regime

In the Haldane mapping of the DSC to the NLSM, the weak coupling regime of the NLSM corresponds to large s spin chains. Thus for the spin $\frac{1}{2}$ system, we cannot access this regime. In the FRC, however, this regime corresponds to the $\kappa_3 \sim \kappa_2 \sim \kappa_4 \gg 1$ region. As we can see from equations (135) and (138), the moment of inertia becomes very large and g very small.

When the moment of inertia is very large, we expect the system to behave semi-classically. To make this explicit, we can scale the euclidean time in Eq. (95), $\tau \rightarrow \sqrt{\kappa_3}\tau$. The action is then written as,

$$S = - \int_{-\infty}^{\infty} d\tau \left[\left(\sum_{I\alpha} \frac{i}{2} \mathbf{A}_{mon}(\hat{\xi}_{I\alpha}) \cdot \partial_\tau \hat{\xi}_{I\alpha} + \frac{\sqrt{\kappa_3} s'^2}{2} \partial_\tau \hat{\xi}_{I\alpha} \cdot \partial_\tau \hat{\xi}_{I\alpha} \right) + \sum_I \left(\frac{\kappa_4}{\kappa_3} \hat{\xi}_{I1} \cdot \partial_\tau^2 \hat{\xi}_{I2} + \frac{\kappa_2}{\kappa_3} \hat{\xi}_{I2} \cdot \partial_\tau^2 \hat{\xi}_{(I+1),1} + \hat{\xi}_{I1} \cdot \hat{\xi}_{I2} + \kappa_1 \hat{\xi}_{I2} \cdot \hat{\xi}_{(I+1),1} \right) \right] \quad (140)$$

The derivation of the NLSM presented in section (VI) can thus be looked upon as the leading order results of a systematic semi-classical expansion, $1/\sqrt{\kappa_3}$ being the expansion parameter.

C. Quantization of the Hall conductance

The above mapping of the fermionic rotor chain onto the nonlinear σ model holds at each step of the renormalization group transformation. Hence, following Eqs. (137) and (138) we can associate a different set of NLSM parameters $g^{(n)}, \theta^{(n)}$ with each set of coupling constants $\kappa_i^{(n)}$ that is defined by the decimation procedure. However, for each step (n) in the decimation procedure the vector field variable \hat{m} is defined for a different lattice constant $a^{(n)} = 2^n(2a) = L(2a)$ or momentum scale $\lambda^{(n)} = \frac{\pi}{a^{(n)}}$. To discuss the limit of scaling we must consider $L \rightarrow \infty$ or, equivalently, large values of n . Specifying to the case $s' = 1/2$ then the quantities $1/g^{(n)}$ and $\theta^{(n)}$ for large values of n approach the fixed point values $1/g = 0$ and $\theta = 2\pi m$ arbitrary closely and are related to one another according to,

$$\left(\frac{1}{g^{(n)}} \right)^2 = (\kappa_3^* + 1) \left| \frac{\theta^{(n)}}{2\pi} - m \right| \propto e^{-2L/\xi}. \quad (141)$$

Here, $m = 0, 1$ and κ_3^* is given by Eq. (121). Notice that the asymptotic form of Eq. (141) defines a different parabola in the $1/g, \theta$ coupling constant plane for each different value of κ_3^* .

Next, in order to make contact with the quantum Hall effect it is convenient to re-express the results of Eq. (134) in terms of the Grassmannian field variable Q .

$$S_{NLSM} = \frac{1}{8} \int_0^\infty dx \int_{-\infty}^\infty d\tau \left[\sigma_{xx}^{(n)} \text{tr} (\partial_\mu Q \partial_\mu Q) + \sigma_{xy}^{(n)} \text{tr} (\epsilon_{\mu\nu} Q \partial_\mu Q \partial_\nu Q) \right], \quad (142)$$

where,

$$\sigma_{xx}^{(n)} = \frac{1}{g^{(n)}} = \mathcal{O}(e^{-L/\xi}), \quad (143)$$

$$\sigma_{xy}^{(n)} = \frac{\theta^{(n)}}{2\pi} = m + \mathcal{O}(e^{-2L/\xi}). \quad (144)$$

Thus at energy scales much less than 1 (note that we are working with $J = 1$) the low energy effective action is precisely equal to the one dimensional action for massless chiral edge excitations, Eq. (19), with k now denoting the *quantized Hall conductance* $\sigma_{xy}^{(n)} = \frac{\theta^{(n)}}{2\pi} = m$. For the semi-infinite system as considered here this one dimensional action is defined along the edge located at $x = 0$.

VII. SUMMARY AND CONCLUSION

We have introduced and investigated the concept of super universality in quantum Hall and quantum spin liquids. This concept has arisen from earlier studies of the $U(N+M)/U(N) \times U(M)$ NLSM's in the physical context of the quantum Hall effect.

The observability and the extreme flatness of the quantum Hall plateaus correspond to the existence of infrared stable fixed points at $\theta = 2\pi k$ as well as the existence of gapless chiral edge excitations at these points. The transitions between adjacent quantum Hall plateaus are generally described by an unstable fixed point located at $\theta = \pi(2k+1)$ which corresponds to a diverging correlation length in the system.

Recent work on the large N CP^{N-1} models have explicitly demonstrated the above super universal features of the instanton vacuum³. In particular, the subtle issue of the existence of a diverging correlation length at $\theta = \pi$ despite the transition being first order was clarified.

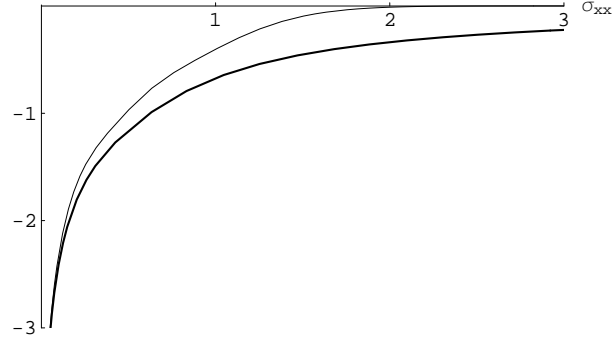


FIG. 8: $2\tilde{\beta}_\sigma$ (bold curve) and $\tilde{\beta}_\theta$ (dashed curve), obtained by interpolating between the strong and weak coupling results, plotted as functions of σ_{xx} .

In this work we have focused on the physics of the strong coupling fixed points at $\theta = 2\pi k$. We first examined the theory in the “bare” strong coupling limit and demonstrated the existence of gapless chiral edge excitations. The edge correlations are independent of the ultraviolet cutoff procedure and also independent of M and N .

We then further concentrated on the $M = N = 1$ case corresponding to the $O(3)$ NLSM. We showed that the edge correlations map on to the correlations of a free spin at the edge. This motivated us to re-examine the Haldane map of DSC to the NLSM treating the edges carefully. We showed how to associate the different geometries of the quantum spin liquid with the quantum Hall liquid with different boundary conditions.

Next we developed a real space renormalization group scheme for the DSC using a combination of path integral and Hamiltonian methods. The technique exploits the fact that under the Haldane mapping the strong coupling regime of the NLSM corresponds to a system of weakly coupled dimers. It is then possible to implement the renormalization group perturbatively in the dimer-dimer coupling. We showed that under renormalization the theory flows away from the DSC to a more complicated theory with four parameters, the FRC. The renormalization procedure was then implemented for the FRC. The recursion relations were obtained to leading order. These were solved exactly demonstrating the existence of the strong coupling fixed points at $\theta = 0$ and 2π . The Haldane map from the FRC to the NLSM then shows that the fixed point action of the instanton vacuum is precisely given by the action for massless chiral edge excitations.

In summary we can say that the FRC, like the large N expansion of the CP^{N-1} model, can be used as an explicit example for demonstrating the *robust quantization* of the Hall conductance. The most important results of this paper are the scaling results of Eqs. (141) and (143) since they describe the strong coupling regime in the σ_{xx} , σ_{xy} conductance plane that previously has not been accessible. These results seem to have a much broader range of validity than considered in this paper. For example, preliminary investigations have shown that the decimation procedure can be extended to include the general case of an $SU(N)$ quantum spin liquid and the Grassmannian $U(2M)/U(M) \times U(M)$ NLSM, yielding basically the same results. These investigations as well as systematic expansion procedures in powers of $1/s$ will be reported in separate papers¹⁷.

To conclude this work we next present the consequences of our results in terms of the global phase diagram for the FRC or, equivalently, the $O(3)$ NLSM. For this purpose we shall make use of the renormalization group results for the weak coupling regime $g \ll 1$ or $\sigma_{xx} \gg 1$ that has previously been obtained from the instanton calculations^{4,16}. We choose to work with the parameters $\sigma_{xx} = 1/g$ and θ . Our scaling results of Eqs. (141) and (143) describing the strong coupling regime can then be obtained as the solutions of the following differential equations,

$$\left. \begin{aligned} \tilde{\beta}_\theta &\equiv \frac{d \ln |\theta - 2\pi m|}{d \ln L} = 2 \ln \sigma_{xx} \\ \tilde{\beta}_\sigma &\equiv \frac{d \ln \sigma_{xx}}{d \ln L} = \ln \sigma_{xx} \end{aligned} \right\} \text{for } \sigma_{xx} \ll 1. \quad (145)$$

On the other hand, from the weak coupling instanton calculations of the $O(3)$ model we have for $\theta \approx 2\pi m$

$$\left. \begin{aligned} \tilde{\beta}_\theta &= -2\pi D_{11} (2\pi \sigma_{xx})^4 e^{-2\pi \sigma_{xx}} \\ \tilde{\beta}_\sigma &= - \left(\frac{1}{\pi \sigma_{xx}} + \frac{1}{(\pi \sigma_{xx})^2} \right) - 2\pi D_{11} (2\pi \sigma_{xx})^4 e^{-2\pi \sigma_{xx}} \end{aligned} \right\} \text{for } \sigma_{xx} \gg 1. \quad (146)$$

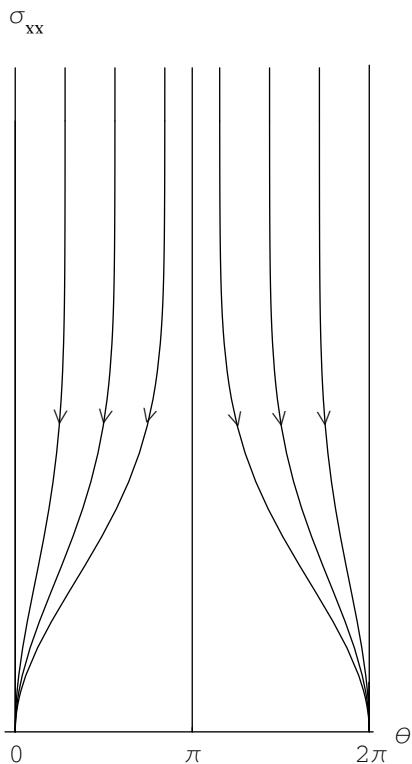


FIG. 9: Renormalization Group flow obtained from the β functions interpolated between the strong and weak coupling results

Here D_{11} is a numerical constant which equals 0.0294. We next can perform a simple numerical interpolation between the asymptotic expressions of Eqs. (145) and (146) to obtain the $\tilde{\beta}$ functions along the entire σ_{xx} axis. This leads to the curves as shown in Fig. 8. Notice that our result for $\tilde{\beta}_\sigma$, which is otherwise well known from the quantum theory of metals, is just the standard way of expressing the phenomenon of *Anderson localization* in two spatial dimensions.¹⁸ The $\tilde{\beta}_\theta$ curve, however, is a generic non-perturbative feature of the instanton vacuum concept and fundamentally describes the formation of the quantum Hall plateaus. From the interpolated $\tilde{\beta}$ functions shown in Fig. 8 we can compute the various different renormalization group flow lines in the σ_{xx}, θ coupling constant plane. These different flow lines which define the *domain of attraction* of the infrared (*quantum Hall*) fixed points $\sigma_{xx} = 0$ and $\theta = 2\pi m$, are shown in Fig. 9. Notice that the results of this paper, notably Fig. 9, provide an important justification of the originally proposed scaling diagram for the $O(3)$ NLSM as shown in Fig. I(b). While the unstable fixed point at $\theta = \pi$ in Fig. I(b) cannot be accessed at the level of approximation that we have implemented in the decimation procedure introduced in this paper, its existence is well known and established¹⁹. We have thus shown that quantum spin liquids, like the quantum Hall liquid, display all the *super universal* strong coupling features of an *instanton vacuum*.

VIII. ACKNOWLEDGMENTS

This research was funded in part by the Dutch National Science Foundations FOM (*Fundamenteel Onderzoek der Materie*) and NWO (*Nederlandse organisatie voor Wetenschappelijk Onderzoek*).

APPENDIX A

Using the change of variables,

$$\hat{\mathbf{n}}_{I1} = \left(1 - \frac{l_I^2}{2}\right) \hat{\mathbf{m}}_I + \mathbf{l}_I, \quad (\text{A1})$$

$$\hat{\mathbf{n}}_{I2} = -\left(1 - \frac{l_I^2}{2}\right) \hat{\mathbf{m}}_I + \mathbf{l}_I, \quad (\text{A2})$$

and expanding to quadratic order in \mathbf{l} , the action in Eq. (56) can be written as,

$$S = \int dt \sum_{I=1}^{\infty} \left(2s^2(1 + \kappa)l_I^2 + \kappa s^2 (\hat{\mathbf{m}}_{(I+1)} - \hat{\mathbf{m}}_{I-1}) \cdot \mathbf{l}_I + 2is \hat{\mathbf{m}}_I \times \partial_t \hat{\mathbf{m}}_I \cdot \mathbf{l}_I - \kappa J s^2 \hat{\mathbf{m}}_I \cdot \hat{\mathbf{m}}_{(I+1)} \right) \quad (\text{A3})$$

In writing the above expression we have made the approximation $\mathbf{l}_I \cdot \mathbf{l}_{(I+1)} \approx (l_I^2 + l_{(I+1)}^2)/2$. This amounts to dropping terms with more than two derivatives in the eventual effective action for the $\hat{\mathbf{m}}$ field. In the next step we integrate out the \mathbf{l} field to obtain the effective action as,

$$S_{eff} = \int dt \left[\kappa s^2 \sum_{I=1}^{\infty} \hat{\mathbf{m}}_I \cdot \hat{\mathbf{m}}_{(I+1)} - \sum_{I=1}^{\infty} \left(4i\kappa s (\hat{\mathbf{m}}_{(I+1)} - \hat{\mathbf{m}}_{I-1}) \cdot \hat{\mathbf{m}}_I \times \partial_t \hat{\mathbf{m}}_I \right. \right. \\ \left. \left. + \kappa^2 s^2 \left((\hat{\mathbf{m}}_{(I+1)} - \hat{\mathbf{m}}_{I-1})^2 - (\hat{\mathbf{m}}_I \cdot (\hat{\mathbf{m}}_{(I+1)} - \hat{\mathbf{m}}_{I-1}))^2 \right) - 4\partial_t \hat{\mathbf{m}}_I \cdot \partial_t \hat{\mathbf{m}}_I \right) \left(8(1 + \kappa) \right)^{-1} \right]. \quad (\text{A4})$$

Taking the continuum limit we get,

$$S_{eff} = \int dt dx \left[\frac{1}{2(1 + \kappa)Ja} \partial_t \hat{\mathbf{m}}(x, t) \cdot \partial_t \hat{\mathbf{m}}(x, t) + \frac{\kappa J s^2 a}{2(1 + \kappa)} \partial_x \hat{\mathbf{m}}(x, t) \cdot \partial_x \hat{\mathbf{m}}(x, t) \right. \\ \left. + \frac{is\kappa}{(1 + \kappa)} \hat{\mathbf{m}}(x, t) \cdot \partial_t \hat{\mathbf{m}}(x, t) \times \partial_x \hat{\mathbf{m}}(x, t) \right]. \quad (\text{A5})$$

where $a/2$ is the lattice spacing.

Dual case

Next we consider the dual case where there is an unpaired spin $\tilde{\mathbf{n}}_E$ at the edge. As before, we first change the variables to $\tilde{\mathbf{m}}$ and \mathbf{l} as given by Eqs. (A1) and (A2). The action in Eq. (58) can then be written as,

$$\tilde{S} = \int dt \left(is\Omega[\tilde{\mathbf{n}}_E] + \kappa J s^2 \tilde{\mathbf{n}}_E \cdot \tilde{\mathbf{m}}_1 + [\kappa s^2 (\tilde{\mathbf{m}}_2 + \tilde{\mathbf{n}}_E) + 2is \tilde{\mathbf{m}}_1 \cdot \partial_t \tilde{\mathbf{m}}_1] \cdot \mathbf{l}_1 + s^2 \left(2 + \kappa - \frac{\kappa}{2} \tilde{\mathbf{n}}_E \cdot \tilde{\mathbf{m}}_1 \right) l_1^2 \right. \\ \left. - \kappa J s^2 \sum_{I=1}^{\infty} \tilde{\mathbf{m}}_I \cdot \tilde{\mathbf{m}}_{(I+1)} + \sum_{I=2}^{\infty} [\kappa s^2 (\tilde{\mathbf{m}}_{(I+1)} - \tilde{\mathbf{m}}_{I-1}) \cdot \mathbf{l}_I + 2is \tilde{\mathbf{m}}_I \times \partial_t \tilde{\mathbf{m}}_I \cdot \mathbf{l}_I + 2s^2(1 + \kappa) l_I^2] \right) \quad (\text{A6})$$

Integrating out \mathbf{l} we obtain the effective action as,

$$\tilde{S}_{eff} = \tilde{S}_{edge} + \tilde{S}_{bulk}, \quad (\text{A7})$$

where,

$$S_{edge} = is\Omega[\tilde{\mathbf{n}}_E] - \kappa s^2 \int dt \left[\tilde{\mathbf{n}}_E \cdot \tilde{\mathbf{m}}_1 - \left(4i\kappa s (\tilde{\mathbf{m}}_2 + \tilde{\mathbf{n}}_E) \cdot \tilde{\mathbf{m}}_1 \times \partial_t \tilde{\mathbf{m}}_1 \right. \right. \\ \left. \left. + \kappa^2 s^2 \left[(\tilde{\mathbf{m}}_2 + \tilde{\mathbf{n}}_E)^2 - (\tilde{\mathbf{m}}_1 \cdot (\tilde{\mathbf{m}}_2 + \tilde{\mathbf{n}}_E))^2 \right] - 4\partial_t \tilde{\mathbf{m}}_1 \cdot \partial_t \tilde{\mathbf{m}}_1 \right) (8 + 4\kappa - 2\kappa \tilde{\mathbf{n}}_E \cdot \tilde{\mathbf{m}}_1)^{-1} \right], \quad (\text{A8})$$

$$S_{bulk} = \int dt \left[\kappa s^2 \sum_{I=1}^{\infty} \tilde{\mathbf{m}}_I \cdot \tilde{\mathbf{m}}_{(I+1)} - \sum_{I=2}^{\infty} \left(4i\kappa s (\tilde{\mathbf{m}}_{(I+1)} - \tilde{\mathbf{m}}_{I-1}) \cdot \tilde{\mathbf{m}}_I \times \partial_t \tilde{\mathbf{m}}_I \right. \right. \\ \left. \left. + \kappa^2 s^2 \left((\tilde{\mathbf{m}}_{(I+1)} - \tilde{\mathbf{m}}_{I-1})^2 - (\tilde{\mathbf{m}}_I \cdot (\tilde{\mathbf{m}}_{(I+1)} - \tilde{\mathbf{m}}_{I-1}))^2 \right) - 4\partial_t \tilde{\mathbf{m}}_I \cdot \partial_t \tilde{\mathbf{m}}_I \right) \left(8(1 + \kappa) \right)^{-1} \right]. \quad (\text{A9})$$

The real part of S_{eff} is minimized by the choice $\tilde{\mathbf{m}}_I(t) = -\tilde{\mathbf{n}}_E$, where we are free to choose $\tilde{\mathbf{n}}_E$. Therefore small fluctuations about the minimum can be described by the slowly varying continuous field $\hat{\mathbf{m}}(x, t)$ with the boundary condition $\hat{\mathbf{m}}(0, t) = -\tilde{\mathbf{n}}_E(t)$. In the continuum limit, $\hat{\mathbf{m}}(x, t) = -\mathbf{m}(x, t)$. Then we obtain the effective dual-action as,

$$\tilde{S}_{eff} = \tilde{S}_{edge} + is \Omega[\hat{\mathbf{m}}(0)] + \int dt dx \left[\frac{1}{2(1 + \kappa)Ja} \partial_t \hat{\mathbf{m}}(x, t) \cdot \partial_t \hat{\mathbf{m}}(x, t) + \frac{\kappa Js^2 a}{2(1 + \kappa)} \partial_x \hat{\mathbf{m}}(x, t) \cdot \partial_x \hat{\mathbf{m}}(x, t) \right. \\ \left. - is \frac{\kappa}{(1 + \kappa)} \hat{\mathbf{m}}(x, t) \cdot \partial_t \hat{\mathbf{m}}(x, t) \times \partial_x \hat{\mathbf{m}}(x, t) \right]. \quad (\text{A10})$$

where,

$$\tilde{S}_{edge} = (4 + 3\kappa)^{-1} \int dt \left[2 \partial_t \hat{\mathbf{m}}(0, t) \cdot \partial_t \hat{\mathbf{m}}(0, t) - 2(\kappa sa)^2 \partial_x \hat{\mathbf{m}}(0, t) \cdot \partial_x \hat{\mathbf{m}}(0, t) \right. \\ \left. + 4is\kappa a \hat{\mathbf{m}}(0, t) \cdot \partial_t \hat{\mathbf{m}}(0, t) \times \partial_x \hat{\mathbf{m}}(0, t) \right]. \quad (\text{A11})$$

S_{edge} is a line integral along the boundary of the space-time and therefore can be written as a bulk integral by applying Stoke's theorem. But this will only result in higher derivative terms and hence can be dropped altogether.

-
- ¹ See e.g. R. Rajaraman, "Solitons and Instantons: An introduction to Solitons and Instantons in Quantum Field Theory", (North-Holland) 1982,
A. M. Polyakov, "Gauge Fields and Strings", (Harwood) 1987.
- ² A.M.M. Pruisken in "The Quantum Hall Effect", eds. R.E. Prange and S.M. Girvin, (Berlin, Springer) (1990).
- ³ A.M.M. Pruisken, M.A. Baranov, and M. Voropaev, cond-mat/0101003, cond-mat/0206011
- ⁴ For a recent review see A.M.M. Pruisken, and I.S. Burmistrov, cond-mat/0407776
- ⁵ A.M.M. Pruisken, B. Škorić, and M.A. Baranov, Phys. Rev. B 60, 16838 (1999).
- ⁶ B. Škorić, and A.M.M. Pruisken, Nucl. Phys. B 559 (1999) 637 and references therein.
- ⁷ E. Witten, Nucl. Phys. B 149 (1979) 285, I. Affleck, Nucl. Phys. B 162 (1980) 461; *ibid* 171 (1980) 420, see also S. Coleman, "Aspects of Symmetry", (Cambridge University Press) 1989.
- ⁸ F. D. M. Haldane, Phys. Lett. **93A**, 464 (1983);
Phys. Rev. Lett. **50**, 1153 (1983).
- ⁹ See I. Affleck in, "Les Houches, Session XLIX, 1988; Fields, Strings and Critical Phenomena, eds. E. Brézin and J. Zinn-Justin", (North-Holland) 1990.
- ¹⁰ Chris J. Hamer, Weihong Zheng and Rajiv R. P. Singh, cond-mat/0307517 and references within.
- ¹¹ D. Controzzi and G. Mussardo, Physical Review Letters **92** 021601, 2004.
- ¹² E. Fradkin, "Field Theories in Condensed Matter Systems", (Addison Wesley) 1991.
- ¹³ A. Perelemov, "Generalized Coherent States and their Applications", (Springer-Verlag) 1986.
- ¹⁴ R. Shankar and N. Read, Nucl. Phys. B **336**, 457 (1990).
- ¹⁵ Naveen Surendran, Ph. D. thesis submitted to the University of Madras, Chennai, India.
- ¹⁶ A.M.M. Pruisken, Nucl. Phys. B **235** 277 (1984), **285** 719 (1987), **290** 61 (1987).
- ¹⁷ A.M.M. Pruisken, R. Shankar and Naveen Surendran, unpublished.
- ¹⁸ E. Abrahams, P. W. Anderson, D. C. Licciardello and T. V. Ramakrishnan, Phys. Rev. Lett. **42**, 673 (1979).
- ¹⁹ See e.g. A. B. Zamolodchikov A.I. B. Zamolodchikov Nucl. Phys. B 379 (1992) 602